JBC RESEARCH ARTICLE

Phosphorylation-dependent interactions of myosin-binding protein C and troponin coordinate the myofilament response to protein kinase A

Received for publication, June 23, 2022, and in revised form, November 23, 2022 Published, Papers in Press, December 5, 2022,
https://doi.org/10.1016/j.jbc.2022.102767

Ivanka R. Sevrieva*, Saraswathi Ponnam, Ziqian Yan, Malcolm Irving, Thomas Kampourakis, and Yin-Biao Sun

From the Randall Centre for Cell and Molecular Biophysics, and British Heart Foundation Centre of Research Excellence, King's College London, London, United Kingdom

Edited by Wolfgang Peti

PKA-mediated phosphorylation of sarcomeric proteins enhances heart muscle performance in response to β-adrenergic stimulation and is associated with accelerated relaxation and increased cardiac output for a given preload. At the cellular level, the latter translates to a greater dependence of Ca^{2+} sensitivity and maximum force on sarcomere length (SL), that is, enhanced length-dependent activation. However, the mechanisms by which PKA phosphorylation of the most notable sarcomeric PKA targets, troponin I (cTnI) and myosin-binding protein C (cMyBP-C), lead to these effects remain elusive. Here, we specifically altered the phosphorylation level of cTnI in heart muscle cells and characterized the structural and functional effects at different levels of background phosphorylation of cMyBP-C and with two different SLs. We found Ser22/23 bisphosphorylation of cTnI was indispensable for the enhancement of length-dependent activation by PKA, as was cMyBP-C phosphorylation. This high level of coordination between cTnI and cMyBP-C may suggest coupling between their regulatory mechanisms. Further evidence for this was provided by our finding that cardiac troponin (cTn) can directly interact with cMyBP-C *in vitro*, in a phosphorylation- and Ca^{2+}-dependent manner. In addition, bisphosphorylation at Ser22/Ser23 increased Ca^{2+} sensitivity at long SL in the presence of endogenously phosphorylated cMyBP-C. When cMyBP-C was dephosphorylated, bisphosphorylation of cTnI increased Ca^{2+} sensitivity and decreased cooperativity at both SLs, which may translate to deleterious effects in physiological settings. Our results could have clinical relevance for disease pathways, where PKA phosphorylation of cTnI may be functionally uncoupled from cMyBP-C phosphorylation due to mutations or haploinsufficiency.

Cardiac troponin (cTn) is the Ca^{2+}-dependent switch in the contractile machinery of heart muscle cells that regulates contraction and relaxation cycles. Ca^{2+} binding to troponin C (cTnC) initiates a series of conformational changes in the troponin complex that release inhibition on actin-myosin interactions. High-resolution crystal structures of troponin and recent advances in electron cryo-microscopy suggested a structural mechanism for thin filament regulation (1, 2). Ca^{2+}-free troponin is elongated, spanning seven actin subunits, and is latched between two tropomyosin strands. This not only restricts their movement, but the C-terminal tail of cardiac troponin I (cTnI) also directly blocks myosin-binding sites on actin. The N-terminal lobe of cTnC (NcTnC), containing the regulatory Ca^{2+} site, is highly dynamic (3). Upon Ca^{2+}-binding, it can bend toward the thin filament surface, to interact with the switch region or switch peptide of cTnI and insert itself between tropomyosin and the flanking regions of cTnI, lifting them away from actin. This rearrangement together with the movement of tropomyosin uncovers the binding sites for myosin heads to allow the formation of actin-myosin crossbridges (2). Strong force-generating crossbridges push the N-lobe, together with the C terminus and inhibitory region of cTnI, further from actin (3). The cyclic ATP-driven interactions propel thin filaments toward the center of the sarcomere during muscle contraction.

Although free calcium concentration is a primary factor controlling sarcomeric function, a number of mechanisms modulate contractile activity by altering the activation state of the thick filaments and mediating interfilament communication (dual filament regulation) (4–7). This enables the heart to adapt rapidly to varying hemodynamic requirements. Within a heartbeat, it can augment its contractile force during ejection following an increase in filling to ensure that it pumps out the same volume it receives. This proportional relationship between stroke volume and ventricular end-diastolic volume is known as the Frank–Starling law of the heart. This law can be extrapolated from the length-tension dependency observed in isolated cardiac muscle cells (8). When heart muscle cells are stretched, they produce a more forceful contraction (9). This phenomenon is largely explained by a cellular mechanism (length-dependent activation or LDA), operating at the level of the myofilaments, that leads to higher Ca^{2+} sensitivity and maximally Ca^{2+}-activated force at longer sarcomere lengths (SLs) (10). LDA is also thought to be mediated by dual filament regulation. At longer SL, the number of force-generating myosin heads is increased through a thick filament–mediated mechanism (11), whereas myofilament

* For correspondence: Ivanka R. Sevrieva, ivanka.r.sevrieva@kcl.ac.uk.

responsiveness to Ca^{2+} is thought to be enhanced *via* structural changes in the thin filament (12–14). However, the signaling pathways and protein–protein interactions underlying these changes are unknown (14–16). Posttranslational modifications in these proteins can modulate LDA (17–20), as can disease-causing mutations (21).

One of the most prominent signaling pathways in the heart is the β-adrenergic pathway, which is associated with adaptation to exercise and the "fight-or-flight" response. Sympathetic activation leads to the release of catecholamines (adrenaline and noradrenaline) that bind to mainly β_1-adrenergic receptors and start a cascade of molecular events (22). The major physiological aspects are increased heart rate (chronotropy), increased contractility (positive inotropy), and faster relaxation (lusitropy). Myofilament LDA is also enhanced (15, 23). At the whole organ level, the contractility of the ventricles increases, and the heart can eject a greater volume of blood for a given end-diastolic volume to accommodate higher perfusion needs. In the cardiomyocyte, rising levels of cyclic AMP activate PKA, which phosphorylates multiple targets: proteins involved in excitation-contraction coupling (sarcolemmal L-type Ca^{2+} channel, phospholamban, and ryanodine receptor) and myofilament proteins (cTnI, cMyBP-C, and titin) (24–26). The functional consequences of PKA treatment in permeabilized cardiac myocyte preparations (Ca^{2+} desensitization, increased relaxation rate, crossbridge kinetics, and LDA) are due to phosphorylation of its myofilament targets. In particular, the individual roles of cTnI and cMyBP-C phosphorylation in response to PKA have been debated over the years, related to the difficulty in distinguishing their relative contributions. Although the controversy has not been resolved, some studies suggest that cTnI phosphorylation by PKA is necessary for reducing myofilament Ca^{2+} sensitivity, speeding up relaxation and enhancing LDA (15, 17, 27–32). However, the specific roles of monophosphorylation *versus* bisphosphorylation at serines 22 and 23 are still unclear (in the literature, these residues are sometimes referred to as serines 23 and 24; the residue numbering used here omits the initial methionine, which is often not present in the mature protein).

The techniques that have been employed to isolate the impact of cTnI on cardiac function typically rely on transgenics, phospho-ablation (serine to alanine S-A substitutions), phosphomimetics (serine to aspartic acid S-D substitutions), or incorporation of the slow skeletal TnI isoform (ssTnI), which lacks the cardiac-specific N-terminal extension, carrying the PKA phosphosites. In the absence of more physiological interventions, these studies provided important information about PKA regulation. However, ssTnI differs from its cardiac counterpart not only in its N-terminus but also in a number of other residues that define isoform-specific functions (33, 34). Moreover, the pseudophosphorylation effects of aspartates have not been examined systematically, although S-D substitutions in N-terminal fragments of cMyBP-C do not fully recapitulate the structural and functional effects of phosphorylating the equivalent serines using PKA (35). Consistent with this, S-D substitutions in the M-domain of C0-C2 N-terminal fragments of cMyBP-C had divergent effects on actin dynamics, which only partially mimicked the effects of genuine phosphorylation (36). Importantly, it has been shown that genuine monophosphorylation at serine 23 of cTnI is sufficient to decrease myofibrillar Ca^{2+} sensitivity, even though this effect had been previously attributed to bisphosphorylation using S-A and S-D substitutions (37–39). It is worth noting that S-A substitutions may not be entirely silent mutations. Introducing changes in the canonical consensus sequence may affect phosphorylation efficiencies. An additional problem with some of the earlier studies was that before the advent of Phos-tag technology, it was not always possible to distinguish between monophosphorylation and bisphosphorylation. This led to some misidentification of the phospho-species (40, 41).

Several protein kinases have been shown to be able to monophosphorylate serine 23: PKA, PKC, PKD, PKG, and most recently the cardiac myosin light chain kinase (cMLCK) (37, 42–44). PKA, PKC isoforms, and PKG can also bisphosphorylate cTnI at Ser22 and Ser23, and the relative proportion of each phospho-species is likely dependent on the strength of the stimulus and the balance between kinase and phosphatase activity. However, serine 23 is an exclusive site for PKD and cMLCK within the protein. In addition, a notable proportion of both monophosphorylated and bisphosphorylated cTnI was identified in fresh transplant human hearts with normal cardiac function (45). Altogether, these findings suggest that phosphorylation of Ser22 and Ser23 may have distinct physiological roles.

The aim of the present work was to examine the impact of genuine Ser22/Ser23 bisphosphorylation on calcium sensitivity and LDA, which is likely to be context specific and linked to the phosphorylation status of other PKA targets. Similar to cTnI, phosphorylation of cMyBP-C by PKA has been proposed to control cardiac muscle LDA (46), and endogenous cMyBP-C is highly phosphorylated in demembranated ventricular trabeculae (47). We used a combination of methodologies: two-way modulation of cTnI phosphorylation by recombinant troponin exchange in demembranated rat heart trabeculae, modulation of the phosphorylation background using *in situ* PKA and lambda protein phosphatase (λPP) treatment, and direct measurement of the cTnI phosphorylation profiles in individual trabeculae in each protocol.

Results

To gain better mechanistic understanding of the functional effects of Ser22/Ser23 bisphosphorylation, we measured structural changes in the thin filament in addition to isometric force during calcium titrations. We used polarized fluorescence from a bifunctional rhodamine (BR) probe attached to the E helix in the C-lobe of cTnC (BR-cTnC-E, Fig. S1) because previous experiments had shown that this probe is sensitive to calcium, switch peptide, and myosin binding but is also affected by SL increase (13, 48). Following whole troponin exchange, BR-cTnC-E was exchanged in a second step with 35% to 50% exchange efficiency (Fig. S2).

Modulation of cTnI and cMyBP-C phosphorylation levels

Rat cardiac troponin complex (cTn) was reconstituted *in vitro*, incubated with PKA to phosphorylate serines 22 and 23 of cTnI and purified to yield 1:1:1 Ser22/23 bisphosphorylated protein complex cTn-2P (Figs. S3–S5). The non-phosphorylated complex (cTn-0P) was prepared by a similar method excluding the phosphorylation step. The troponin complexes were exchanged into demembranated rat ventricular trabeculae by overnight soak in relaxing buffer containing protein kinase/phosphatase inhibitors. The troponin exchange protocol is specific for cardiac troponin and does not change the abundance or phosphorylation level of other sarcomeric proteins (Fig. S6) and is therefore a tailored intervention to modulate cTnI phosphorylation at the PKA sites Ser22 and Ser23 *in situ*.

The trabeculae were either untreated and reconstituted with one of the troponin complexes (untreated, cTn-0P or untreated, cTn-2P) or pretreated with a lambda protein phosphatase (λPP) to reduce myofilament phosphorylation background and then exchanged with one of the troponin complexes (λPP, cTn-0P and λPP, cTn-2P). Since λPP treatment is a nonspecific intervention, an additional control group of trabeculae was λPP treated and then back-phosphorylated with the catalytic subunit of PKA to identify any effects of other PKA targets such as cMyBP-C. This group was reconstituted with bisphosphorylated cTn overnight (λPP, PKA, cTn-2P).

We also determined cMyBP-C phosphorylation in untreated and λPP-treated demembranated heart samples (Fig. 1). The amount of cMyBP-C that could be extracted from single trabeculae was insufficient to characterize cMyBP-C phosphorylation. Therefore, we prepared rat cardiac myofibrils (CMFs) from the remaining heart tissue and subjected them to the same treatments as the trabeculae. cMyBP-C phosphorylation level was assessed using the intensity of the Pro-Q Diamond phosphoprotein stain relative to the total SYPRO Ruby stain (Fig. 1*A*). We also used the Western blot signal from the phospho-specific antibody against Ser282-phosphorylated cMyBP-C divided by the signal from a phosphorylation-independent anti-cMyBP-C antibody (G-7, Fig. 1*B*). These intensities were normalized to those before λPP and PKA treatment ("Pre" in Fig. 1*C*). The basal level of cMyBP-C phosphorylation at the main PKA site (Ser282) was high in our heart preparation (Fig. 1*C*). Incubation with λPP

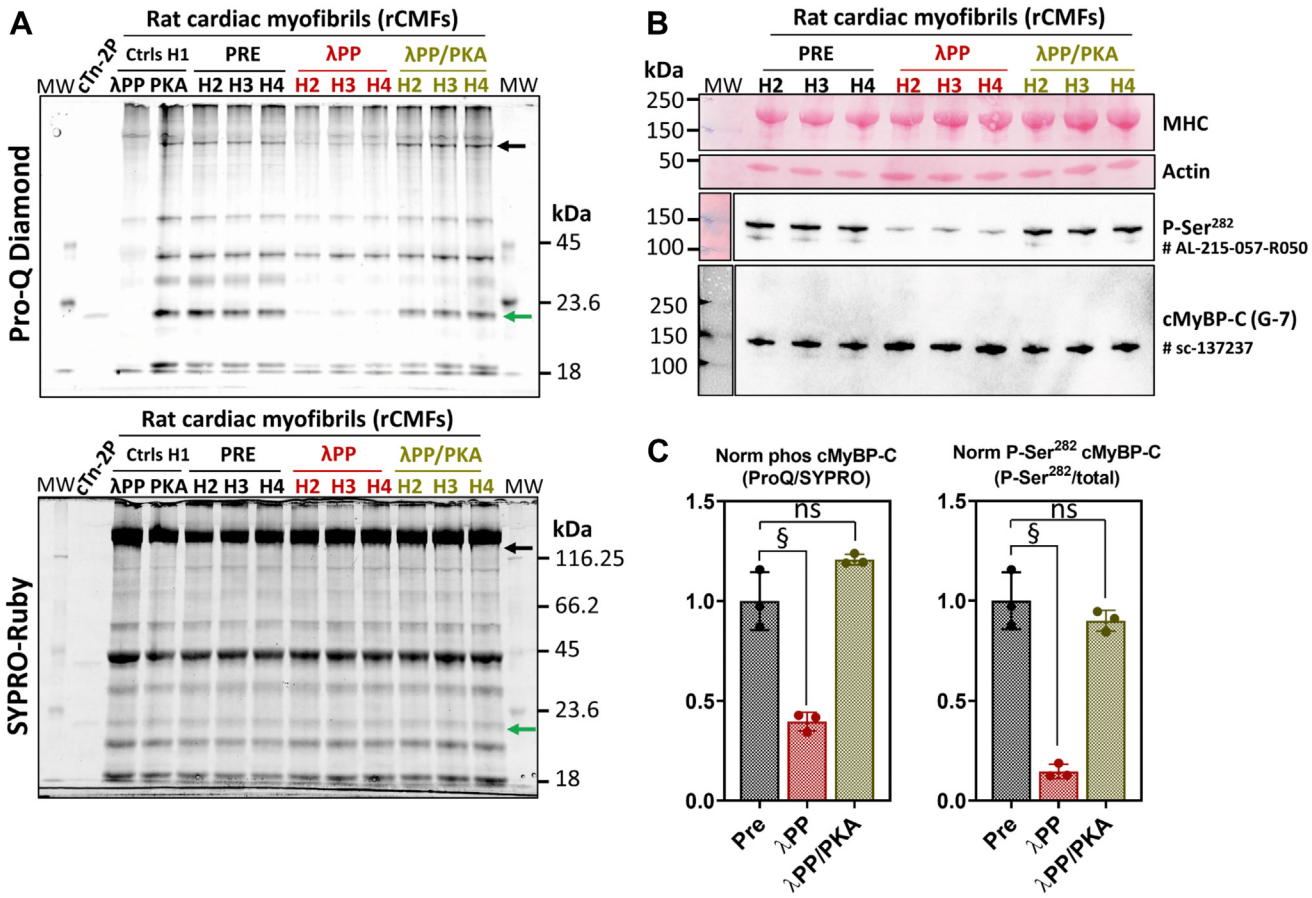

Figure 1. Effects of λPP and PKA treatment on myofilament protein phosphorylation levels. *A*, pro-Q Diamond phospho-protein (*top*) and SYPRO-Ruby total protein staining (*bottom*) of cardiac myofibrils (CMFs) isolated from three different hearts before (PRE), after λPP, and after λPP/PKA-treatment. The position of cMyBP-C and cTnI are indicated by *black* and *green arrows*, respectively. *B*, cMyBP-C phosphorylation levels were determined by Western blot using phosphoserine 282–specific and total cMyBP-C antibodies. *C*, relative cMyBP-C phosphorylation levels determined by Pro-Q/SYPRO staining (*left*) and Western blot (*right*) of samples before treatment (PRE) and after λPP and λPP/PKA treatment. Bar plots are means ± SD. Comparisons with (PRE) were done using Brown-Forsythe and Welch ANOVA and Dunnett T3 test ($^{\S}p < 0.05$).

reduced cMyBP-C phosphorylation, and PKA treatment restored it to the basal level.

The phosphorylation level of troponin I was measured in individual trabeculae, harvested after experiments from all five intervention groups, using Phos-tag-SDS-PAGE and Western blotting against cTnI (Fig. 2*A*). Troponin I phosphorylation level was also measured in ventricular tissue samples treated with the same protocols (Fig. S7) because some trabeculae were too small to allow reliable measurement of the extent of cTnI phosphorylation. Phos-tag decreases the mobility of phosphoproteins, so that from top to bottom the major bands correspond to bisphosphorylated cTnI, monophosphorylated cTnI, and nonphosphorylated cTnI, respectively. The total cTnI phosphorylation (mols incorporated phosphate per mol cTnI, mol Pi/mol cTnI) is similar in trabeculae (Fig. 2*B*) and time-matched ventricular tissue samples (Fig. S7) in all five groups. The relative percentage of each species in the experimental trabeculae is also shown in Figure 2, *C* and *D*. The protocols used here produced a large increase in the fraction of bisphosphorylated cTnI in trabeculae exchanged with cTn-2P compared to cTn-0P, although some nonphosphorylated and monophosphorylated cTnI species were present in all groups. cTnI degradation, detected below the nonphosphorylated band, was less than 10% for all groups except λPP, cTn-0P (∼16%). Troponin I bisphosphorylation levels in λPP-treated trabeculae that had been reconstituted with either nonphosphorylated or bisphosphorylated troponin complexes (cTn-0P and cTn-2P) were almost identical to those in trabeculae that had not been treated with λPP (Fig. 2*D*).

cTnI bisphosphorylation increases myofilament Ca^{2+} sensitivity

In trabeculae exchanged with cTn-0P, stretch from SL 1.9 μm to SL 2.3 μm increased the Ca^{2+} sensitivity of force, as reported by pCa_{50}, the negative logarithm of the calcium concentration resulting in half-maximal activation (Table 1 and Fig. 3*A*, SL 1.9 μm solid black line and open black circles and SL 2.3 μm solid black line and closed black circles).

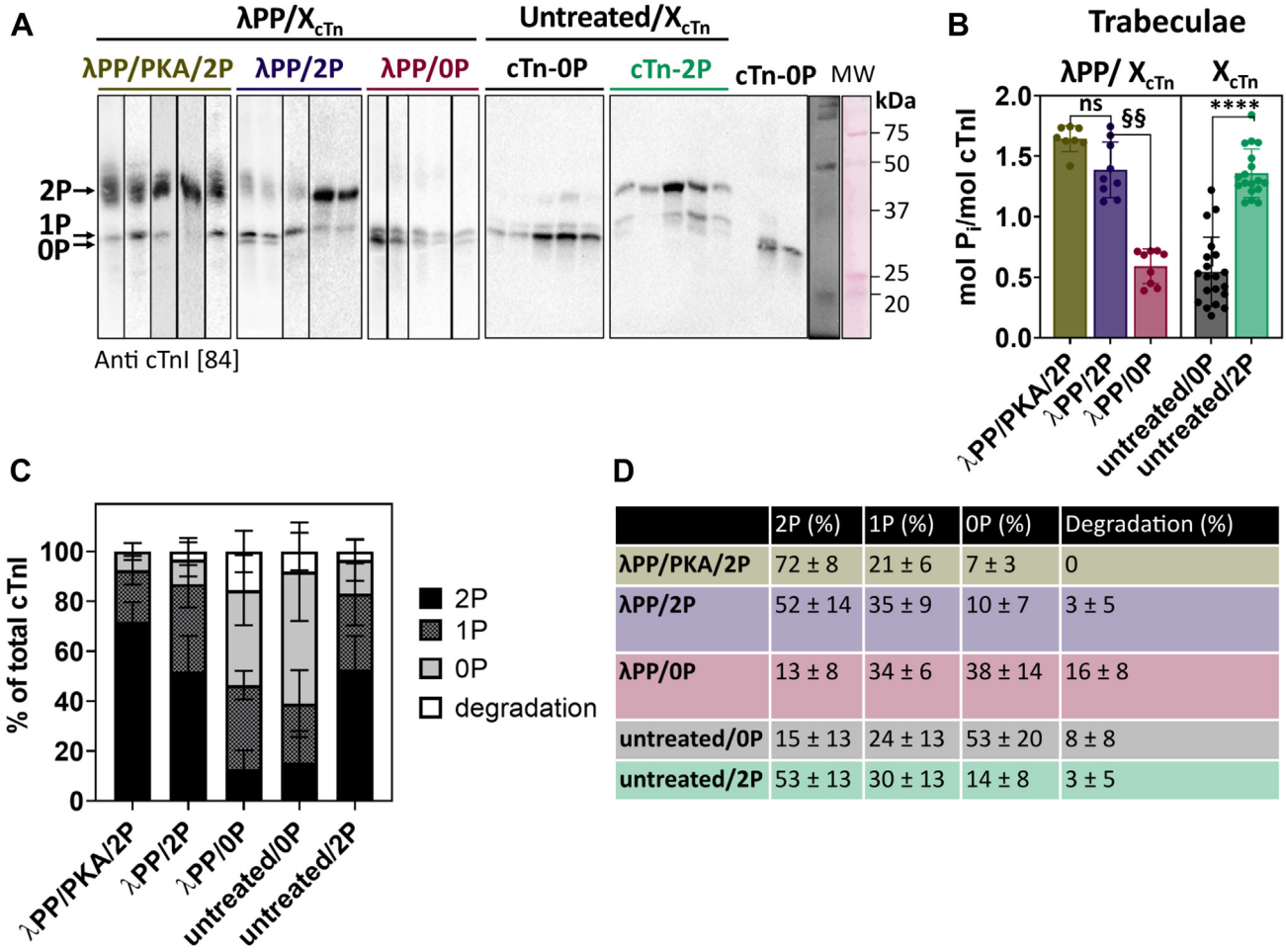

	2P (%)	1P (%)	0P (%)	Degradation (%)
λPP/PKA/2P	72 ± 8	21 ± 6	7 ± 3	0
λPP/2P	52 ± 14	35 ± 9	10 ± 7	3 ± 5
λPP/0P	13 ± 8	34 ± 6	38 ± 14	16 ± 8
untreated/0P	15 ± 13	24 ± 13	53 ± 20	8 ± 8
untreated/2P	53 ± 13	30 ± 13	14 ± 8	3 ± 5

Figure 2. Modulation of cardiac troponin I phosphorylation in ventricular trabeculae by recombinant troponin exchange. *A*, example Phos-tag-Western blots against cTnI from experimental ventricular trabeculae, either untreated or λPP-treated, followed by exchange with either nonphosphorylated or bisphosphorylated recombinant rat troponin complex. Troponin I was detected with the mouse monoclonal antibody 84 against the central region (residues 118–127 in the rat cardiac sequence). *B*, densitometric analysis and plots of mol incorporated phosphate per mol cTnI (mol Pi/mol cTnI). *C*, densitometric analysis of cTnI phosphorylation levels from single trabeculae showing the relative percentages of cTnI species, summarized in (*D*). Bar plots are means ± SD. Statistics in (*B*) are Kruskal–Wallis test with Dunn's multiple comparisons test against the λPP-treated cTn-2P group (ns not significant, $^{§§}p < 0.01$) and unpaired two-tailed *t* test for the untreated groups (****$p < 0.0001$).

Table 1
Summary of force-pCa parameters for untreated and λPP-treated rat ventricular trabeculae

		$F_{passive}$ (mN/mm^2)	F_{max} (mN/mm^2)	$F_{pCa\ 5.9}$ (mN/mm^2)	pCa_{50}	ΔpCa_{50}	n_H
Untreated cTn-0P	SL 1.9 μm N = 8, n = 15	0.6 ± 1.1	34 ± 11	1 ± 1.2	5.72 ± 0.05	0.10 ± 0.03***	11.5 ± 3.1
	SL 2.3 μm N = 8, n = 12	19 ± 13†††	66 ± 22†††	18 ± 8.8†*	5.82 ± 0.06†††**		10.4 ± 3.5
Untreated cTn-2P	SL 1.9 μm N = 7, n = 14	0.3 ± 0.2	36 ± 17	3 ± 4	5.75 ± 0.05	0.15 ± 0.04	10.6 ± 2.1
	SL 2.3 μm N = 6, n = 11	16 ± 11†††	73 ± 37†††	50 ± 34††	5.90 ± 0.06†††		8.4 ± 2.7†
λPP cTn-0P	SL 1.9 μm N = 7, n = 9	2.7 ± 1.9	40 ± 18	4 ± 4$^{\$}$	5.77 ± 0.03$^{\$\$}$	0.10 ± 0.02	9.0 ± 2.2$^{\$}$
	SL 2.3 μm N = 7, n = 9	21 ± 12††	68 ± 23†††	27 ± 15†††	5.88 ± 0.03$^{\dagger\dagger\dagger\$\$}$		7.1 ± 1.7$^{\dagger\$\$\$}$
λPP cTn-2P	SL 1.9 μm N = 7, n = 10	2.5 ± 1.6	34 ± 10	9 ± 6	5.83 ± 0.05	0.11 ± 0.03	6.7 ± 1.4
	SL 2.3 μm N = 7, n = 8	23 ± 13††	68 ± 22†††	41 ± 20†††	5.94 ± 0.06†††		4.3 ± 0.7†††
λPP PKA cTn-2P	SL 1.9 μm N = 6, n = 9	1.2 ± 0.6$^{\$}$	42 ± 8	8 ± 5	5.82 ± 0.04	0.15 ± 0.02$^{\$\$}$	8.5 ± 2.3
	SL 2.3 μm N = 6, n = 9	28 ± 15††	73 ± 16†††	49 ± 15†††	5.97 ± 0.03†††		6.0 ± 1.4$^{\dagger\dagger\$}$

N = number of hearts, n = number of experiments. Means ± SD. Statistics are described in more detail in the Experimental procedures.
*$p < 0.05$ in unpaired two-tailed comparisons between the untreated cTn-0P and cTn-2P groups.
**$p < 0.01$ in unpaired two-tailed comparisons between the untreated cTn-0P and cTn-2P groups.
***$p < 0.001$ in unpaired two-tailed comparisons between the untreated cTn-0P and cTn-2P groups.
$^{\$}p < 0.05$ in two-tailed comparisons of the λPP, cTn-0P and λPP, PKA, cTn-2P groups against the λPP, cTn-2P group.
$^{\$\$}p < 0.01$ in two-tailed comparisons of the λPP, cTn-0P and λPP, PKA, cTn-2P groups against the λPP, cTn-2P group
$^{\$\$\$}p < 0.001$ in two-tailed comparisons of the λPP, cTn-0P and λPP, PKA, cTn-2P groups against the λPP, cTn-2P group.
$^{\dagger}p < 0.05$ in paired comparisons between SL 1.9 μm and 2.3 μm.
$^{\dagger\dagger}p < 0.01$ in paired comparisons between SL 1.9 μm and 2.3 μm.
$^{\dagger\dagger\dagger}p < 0.001$ in paired comparisons between SL 1.9 μm and 2.3 μm.

This length-dependent effect on Ca^{2+} sensitivity was also observed in trabeculae exchanged with cTn-2P (Table 1 and Fig. 3*B*, 1.9 μm solid green line and open green circles and 2.3 μm solid green line and closed green circles). In contrast to most previous reports (38, 39), we found that at short SL (1.9 μm) increasing cTnI bisphosphorylation did not reduce the Ca^{2+} sensitivity of force (Table 1 and Fig. 3*B* solid green line and open circles compared to the dashed black line). Untreated trabeculae reconstituted with cTn-2P had higher Ca^{2+} sensitivity at SL 2.3 μm compared to their cTn-0P counterparts, that is, the force-pCa relation was shifted to the left with respect to that of the cTn-0P group (Fig. 3*B*, solid green line and closed circles compared to the dotted black line, Table 1). This led us to hypothesize that the functional role of bisphosphorylation might be to enhance the length-dependent shift in calcium sensitivity under specific conditions rather than to desensitize the myofilament to calcium.

The Ca^{2+}-sensitizing effect of increasing SL was also seen in trabeculae treated with λPP and reconstituted with cTn-0P (Fig. 3*C*, SL 1.9 μm solid red line and open red circles and SL 2.3 μm solid red line and closed red circles). Similarly, the length-dependent shift in the force–pCa curve was observed in λPP-treated trabeculae exchanged with cTn-2P (Fig. 3*D*, SL 1.9 μm solid blue line and open blue circles and SL 2.3 μm solid blue line and closed blue circles). However, λPP-treated trabeculae exchanged with cTn-2P had higher Ca^{2+} sensitivity at both short (SL 1.9 μm) and long SLs (SL 2.3 μm) compared to the λPP-treated, cTn-0P group (Fig. 3*D*, SL 1.9 μm solid blue line and open blue circles compared to the dashed red line, SL 2.3 μm solid blue line and closed blue circles compared to the dotted red line, Table 1).

Phosphorylation of both cTn and cMyBP-C controls LDA and cooperativity in cardiac muscle

In untreated, cTn-0P trabeculae, increasing SL from 1.9 to 2.3 μm not only significantly increased the Ca^{2+} sensitivity of force development but also the maximal calcium-activated isometric force (Table 1). Exchange of cTn-2P into demembranated untreated trabeculae resulted in a significantly larger ΔpCa_{50} due to sarcomere lengthening without affecting the maximal force at pCa 4.5 (Table 1). In intact heart muscle, the diastolic and systolic free intracellular calcium concentration $[Ca^{2+}]_i$ depends on stimulation frequency and the presence of β-adrenergic agonists and is typically in the range 70 to 250 nmol/l for diastole (pCa 6.6–7.2) and 0.5 to 1.5 μmol/l (pCa 5.8–6.2) for systole (49–54). At pCa 5.9, which is close to the free calcium concentration in systole, force at the longer SL was much higher in the cTn-2P group than in the cTn-0P group (Table 1).

The aforementioned experiments indicated that the shift in Ca^{2+} sensitivity associated with LDA (ΔpCa_{50}) can be enhanced by cTnI bisphosphorylation in demembranated trabeculae. We wanted to know whether this effect was influenced by the level of phosphorylation of other proteins, in particular cMyBP-C. Therefore, we treated trabeculae with λPP, which dephosphorylates cMyBP-C, as described earlier. At both short and long SLs, λPP-treated trabeculae had similar maximum force as untreated trabeculae (Table 1). ΔpCa_{50} for

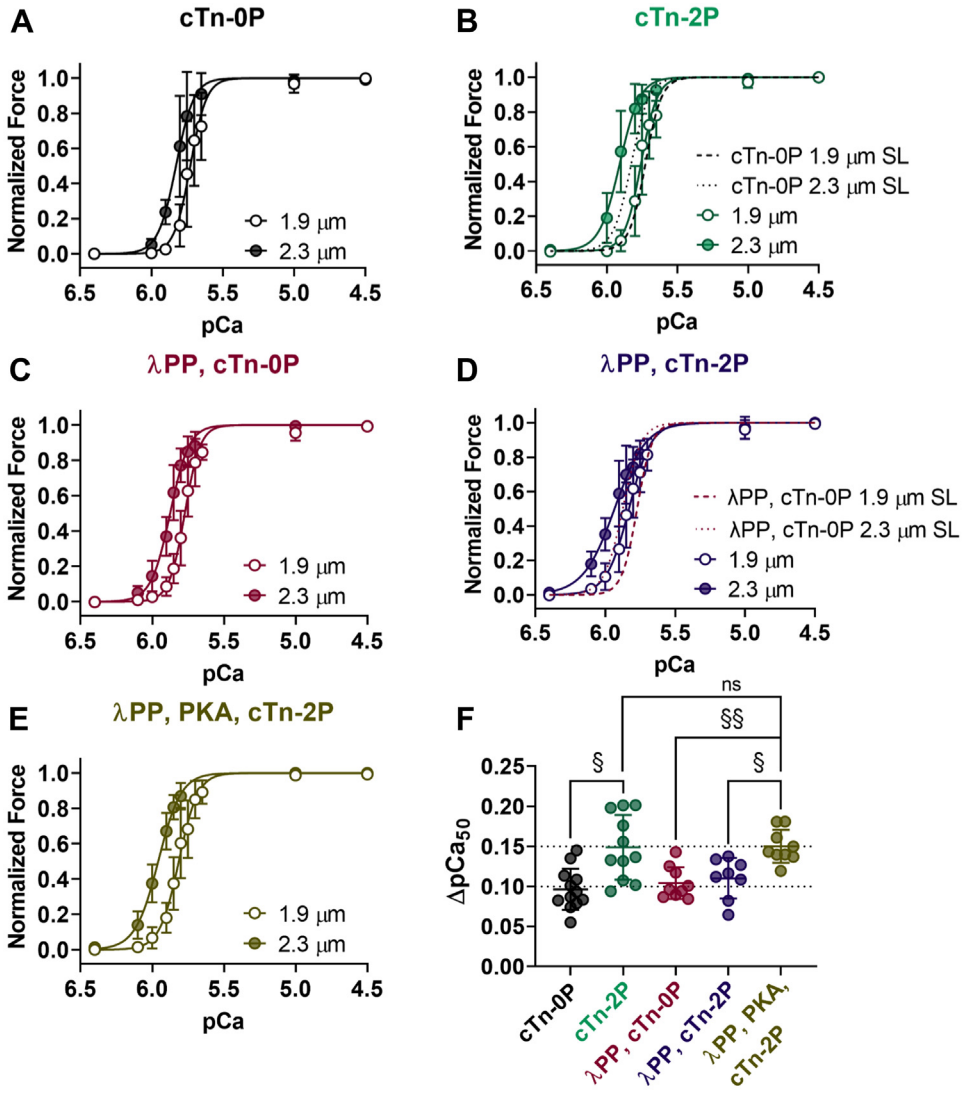

Figure 3. cTnI and cMyBP-C phosphorylation control cardiac length-dependent activation. Force-calcium titration of untreated (*A* and *B*) and λPP-treated trabeculae (*C* and *D*) exchanged with either nonphosphorylated (*A* and *C*) or bisphosphorylated cTn complex (*B* and *D*) at short (1.9 μm, open symbols) and long sarcomere length (2.3 μm, closed symbols). The dotted and *dashed lines* in (*B*) and (*D*) represent the Hill fits shown in (*A*) and (*C*), respectively. *E*, force-calcium relation of λPP-treated and subsequently PKA-treated trabeculae exchanged with bisphosphorylated cTn at short and long sarcomere length. *F*, summary plot showing the increase in calcium sensitivity (ΔpCa_{50}) upon sarcomere length increase for all experimental groups. Means ± SD, (*A*) n = 12 to 15, (*B*) n = 11 to 14, (*C*) n = 9, (*D*) n=8 to 10, and (*E*) n = 9. Statistical significance of differences was assessed with Brown-Forsythe and Welch ANOVA, followed by Dunnett's T3 multiple comparisons test: ns not significant, $^{\S}p < 0.05$ and $^{\S\S}p < 0.01$.

force in λPP-treated trabeculae exchanged with cTn-0P with low cTnI and cMyBP-C phosphorylation levels was not significantly different from that of the untreated cTn-0P group with highly phosphorylated cMyBP-C (Fig. 3*C* vs. Fig. 3*A* and Table 1). We conclude that LDA is not sensitive to the level of cMyBP-C phosphorylation in conditions in which cTnI is only 13% to 15% bisphosphorylated.

Exchange of cTn-2P into λPP-dephosphorylated trabeculae increased the Ca^{2+} sensitivity of force at the short and long SLs to the same extent, so that ΔpCa_{50} was not enhanced compared to the λPP, cTn-0P group (Fig. 3*D* and Table 1). These results suggest that cMyBP-C dephosphorylation blunts the effects of cTnI bisphosphorylation on LDA.

To test for unspecific effects of incubation of demembranated myocardium with λPP, we first dephosphorylated trabeculae from the same heart with λPP, then phosphorylated *in situ* with PKA before exchanging overnight with cTn-2P. As mentioned earlier, this protocol restored the cMyBP-C phosphorylation level to that observed before λPP treatment. These PKA back-phosphorylated trabeculae with high cMyBP-C phosphorylation levels had a higher ΔpCa_{50} (Fig. 3*E* and Table 1), similar to that of untreated trabeculae exchanged with cTn-2P (Fig. 3*F*). Although the mean level of cTnI bisphosphorylation was higher in λPP-treated/PKA back-phosphorylated trabeculae compared to the λPP-treated cTn-2P group, the difference was not statistically significant (Fig. 2*B*). Moreover, increasing cTnI bisphosphorylation was insufficient to increase ΔpCa_{50} in the absence of PKA. Therefore, it is unlikely that the increase in ΔpCa_{50} in this group was due to cTnI alone.

Reconstitution of untreated trabeculae with cTn-2P had no impact on the cooperativity of the force-pCa relation, as

determined by the Hill coefficient n_H, at either the short or long length compared to cTn-0P (Table 1). However, in the cTn-2P trabeculae n_H was reduced by stretching to the longer SL (Table 1). The relatively high values for n_H reported here are most likely due to the stepwise calcium titration protocol used (see Experimental procedures). At both the short and long SLs, λPP-treated trabeculae had lower n_H compared to untreated trabeculae and there was a further decrease after increasing SL (Table 1). n_H was significantly lower in the λPP, cTn-2P group compared to the λPP, cTn-0P group at both the short and long SLs and PKA treatment reversed this effect (Table 1). These results suggest that cTnI and cMyBP-C phosphorylation can regulate myofilament cooperativity, working together rather than independently.

Correlation of Ca^{2+} sensitivity and ΔpCa_{50} with cTnI bisphosphorylation

The comparisons between the cTn-0P and cTn-2P groups reported previously cannot be interpreted solely in terms of bisphosphorylation because the troponin exchange protocol results in mixed populations of nonphosphorylated, monophosphorylated, and bisphosphorylated troponin I (Fig. 2*D*). Therefore, we looked at whether the increase in Ca^{2+} sensitivity of force and the SL dependence of pCa_{50} (ΔpCa_{50}), which is often used as a measure of LDA, correlated with the measured percentage of bisphosphorylated cTnI in trabeculae (Fig. 4). We were also interested in any influence of PKA phosphorylation background on these relationships.

In trabeculae with the high basal level of cMyBP-C phosphorylation, the calcium sensitivity of force at the short SL was not significantly correlated with the fraction of bisphosphorylated cTnI (r = 0.290 and p = 0.09, Fig. 4*A*). However, at the long SL, there was a significant correlation between the two variables (r = 0.651 and p = 0.0001, Fig. 4*B*). ΔpCa_{50} was also significantly correlated with the fraction of bisphosphorylated cTnI (r = 0.674 and $p < 0.0001$, Fig. 4*C*), suggesting that cTnI bisphosphorylation may be responsible for the enhanced LDA following PKA treatment.

In λPP-treated trabeculae, in which cMyBP-C was dephosphorylated, pCa_{50} was significantly correlated with the fraction of bisphosphorylated cTnI at the short SL (r = 0.508 and p =

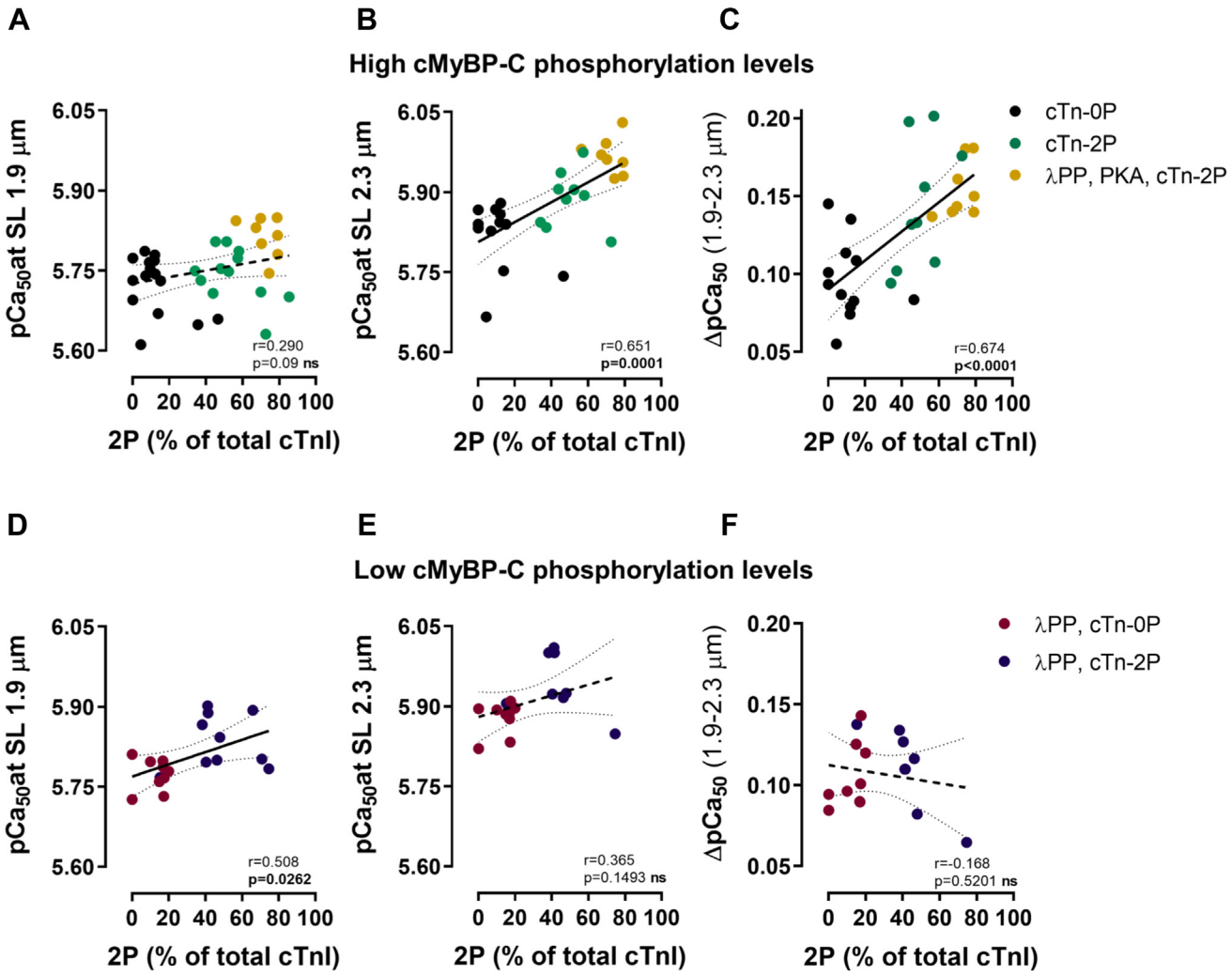

Figure 4. Pearson correlation analysis of force pCa_{50} and ΔpCa_{50} *versus* the percentage Ser22/23 bisphosphorylated cTnI. *A*, *B*, and *C*,: data from trabeculae with high levels of cMyBP-C phosphorylation. *D* and *E*, and *F*, data from λPP-treated trabeculae with low levels of cMyBP-C phosphorylation.

0.0262, Fig. 4*D*) but not at the long SL (r = 0.365 and p = 0.1493, Fig. 4*E*). In contrast with the clear effect seen with basal levels of cMyBP-C phosphorylation (Fig. 4*C*), there was no significant correlation between ΔpCa_{50} and cTnI bisphosphorylation level when trabeculae were dephosphorylated by λPP (Fig. 4*F*), suggesting that the effect of bisphosphorylated cTnI on LDA depends on the cMyBP-C phosphorylation background.

Structural changes in troponin

In the protocols described previously, we also monitored the structural changes in the IT arm, a troponin domain comprising of the C-terminal lobe of cTnC (CcTnC) sandwiched between the first α-helix of cTnI and the second α-helix of cTnT, which forms a coiled-coil with the second cTnI α-helix (Fig. S1). We used a bifunctional rhodamine probe attached along the E helix of cTnC (BR-cTnC-E, Fig. S1), which has been shown to be sensitive to calcium and switch peptide binding and strong myosin crossbridges (13, 47, 48, 55). Changes in the orientation of this probe correlate with the activation state of the thin filaments. Probe orientation is reported as the order parameter P_2, which describes the *in situ* orientation of the probe with respect to the trabecular or thin filament axis, where P_2 would be +1 if all the probes were parallel to the filament axis and -0.5 if they were all perpendicular (Fig. S1). The parameters extracted from the Hill fits of the P_2 data in Figure 5 are summarized in Table 2.

Increasing SL increased P_2 at low and high calcium. This effect had the same direction as the P_2 change associated with switching off the thin filament, albeit not the same magnitude (Fig. 5 and Table 2). It could be in part due to the better alignment of myofibrils at the long SL. The shift in P_2 was slightly bigger at diastolic calcium concentration (pCa 7.0-pCa

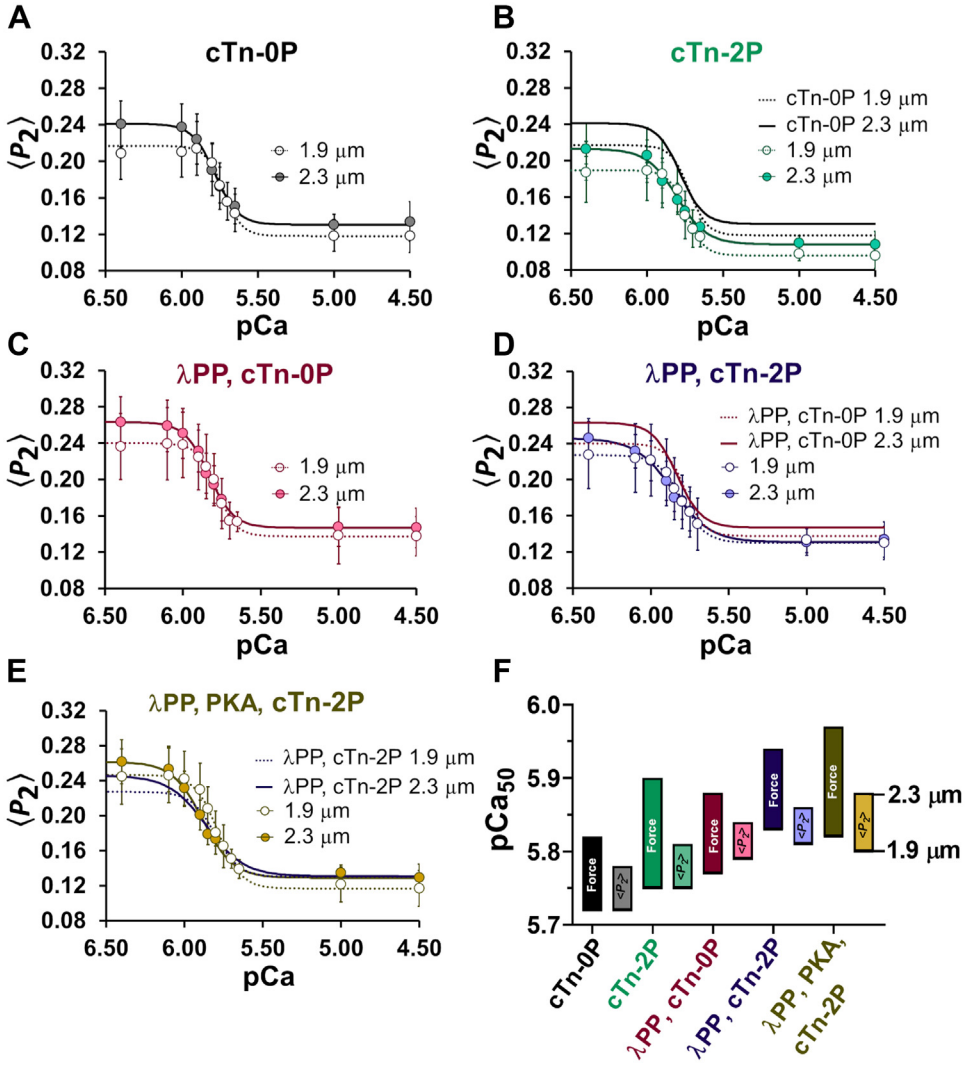

Figure 5. Structural changes in troponin. P_2-calcium titrations of untreated (*A* and *B*) and λPP-treated trabeculae (*C* and *D*) exchanged with either nonphosphorylated (*A* and *C*) or bisphosphorylated cTn complex (*B* and *D*) at short (1.9 μm, open symbols) and long sarcomere length (2.3 μm, closed symbols). *Dotted lines* are Hill fits at short sarcomere length and solid lines are Hill fits at long sarcomere length. *E*, P_2-calcium relation of λPP-treated and subsequently PKA-treated trabeculae exchanged with bisphosphorylated cTn at short and long sarcomere length. *F*, plot of pCa_{50} (means) of force (*dark colors*) and P_2 (*light colors*) at the two sarcomere lengths as indicated on the right. Means ± SD, (*A*) n = 12 to 15, (*B*) n = 11 to 14, (*C*) n = 9, (*D*) n=8 to 10, and (*E*) n = 9.

Table 2
Summary of P_2-pCa parameters for untreated and λPP-treated rat ventricular trabeculae

		P_2 *pCa 9.0*	P_{2min} *max* $[Ca^{2+}]$	P_{2max}	A (P_{2max} – P_{2min})	pCa_{50}	ΔpCa_{50}	n_H
Untreated cTn-0P	SL 1.9 μm N = 8, n = 15	0.19 ± 0.03	0.12 ± 0.02***	0.21 ± 0.03	0.09 ± 0.02	5.72 ± 0.04	0.060 ± 0.017	9.0 ± 2.1
	SL 2.3 μm N = 8, n = 12	0.22 ± 0.02†††*	0.13 ± 0.02†††*	0.24 ± 0.03†††**	0.11 ± 0.01†††	5.78 ± 0.05†††		7.2 ± 1.7††**
Untreated cTn-2P	SL 1.9 μm N = 7, n = 14	0.17 ± 0.03	0.10 ± 0.01	0.19 ± 0.03	0.09 ± 0.03	5.75 ± 0.04	0.064 ± 0.028	9.7 ± 1.9
	SL 2.3 μm N = 6, n = 11	0.19 ± 0.03†††	0.11 ± 0.01†††	0.21 ± 0.03†††	0.11 ± 0.02††	5.81 ± 0.05†††		5.3 ± 1.1†††
λPP cTn-0P	SL 1.9 μm N = 7, n = 9	0.22 ± 0.04	0.14 ± 0.02	0.24 ± 0.04	0.10 ± 0.02	5.79 ± 0.04	0.05 ± 0.03	7.0 ± 1.4
	SL 2.3 μm N = 7, n = 9	0.25 ± 0.03††	0.15 ± 0.02††	0.26 ± 0.03†	0.12 ± 0.01†	5.84 ± 0.02†††		5.7 ± 1.0††
λPP cTn-2P	SL 1.9 μm N = 7, n = 10	0.21 ± 0.04	0.13 ± 0.02	0.23 ± 0.04	0.10 ± 0.03	5.81 ± 0.03	0.06 ± 0.03	5.9 ± 1.7
	SL 2.3 μm N = 7, n = 8	0.24 ± 0.02††	0.13 ± 0.01	0.25 ± 0.02††	0.11 ± 0.02††	5.86 ± 0.04†††		4.6 ± 1.0†
λPP PKA cTn-2P	SL 1.9 μm N = 6, n = 9	0.23 ± 0.03	0.12 ± 0.02	0.25 ± 0.03	0.12 ± 0.02	5.80 ± 0.03	0.08 ± 0.02	7.5 ± 2.0
	SL 2.3 μm N = 6, n = 9	0.25 ± 0.03†††	0.13 ± 0.01††	0.26 ± 0.03††	0.13 ± 0.02††	5.88 ± 0.02†††		5.0 ± 1.0††

A is the amplitude of structural change or the difference between the top and bottom of the curve (maximum P_2 value at maximal calcium concentration and the minimum P_2 value at p Ca5.9-pCa 6.4). N = number of hearts, n = number of experiments. Means ± SD. The statistics are described in more detail in the Experimental procedures.
*$p < 0.05$ in unpaired two-tailed comparisons between the untreated cTn-0P and cTn-2P groups.
**$p < 0.01$ in unpaired two-tailed comparisons between the untreated cTn-0P and cTn-2P groups.
***$p < 0.001$ in unpaired two-tailed comparisons between the untreated cTn-0P and cTn-2P groups.
$^{\$}p < 0.05$ in two-tailed comparisons of the λPP, cTn-0P and λPP, PKA, cTn-2P groups against the λPP, cTn-2P group.
$^{\$\$}p < 0.01$ in two-tailed comparisons of the λPP, cTn-0P and λPP, PKA, cTn-2P groups against the λPP, cTn-2P group
$^{\$\$\$}p < 0.001$ in two-tailed comparisons of the λPP, cTn-0P and λPP, PKA, cTn-2P groups against the λPP, cTn-2P group.
$^{\dagger}p < 0.05$ in paired comparisons between SL 1.9 μm and 2.3 μm
$^{\dagger\dagger}p < 0.01$ in paired comparisons between SL 1.9 μm and 2.3 μm
$^{\dagger\dagger\dagger}p < 0.001$ in paired comparisons between SL 1.9 μm and 2.3 μm.

6.4) than at maximal activation (pCa 4.5), leading to a small but reproducible increase in the amplitude of structural change at the long SL in all experimental groups (Table 2).

Exchange of untreated trabeculae with cTn-2P decreased P_2 at all $[Ca^{2+}]$ compared to trabeculae exchanged with cTn-0P (Fig. 5*A versus* Fig. 5*B*, SL 1.9 μm dotted black line *versus* dotted green line and SL 2.3 μm solid black line *versus* solid green line). During calcium activation, there is a much larger decrease in P_2, which is related to switching on the thin filament as mentioned earlier (48). In the λPP set of experiments, the effect of cTn-2P on P_2 was not statistically significant (Fig. 5*C versus* Fig. 5*D*, SL 1.9 μm dotted red line *versus* dotted blue line and SL 2.3 μm solid red line *versus* solid blue line). Back-phosphorylation with PKA did not significantly change P_2 compared to the λPP, cTn-2P group (Fig. 5*D versus* Fig. 5*E*, SL 1.9 μm dotted blue line *versus* dotted yellow green line and SL 2.3 μm solid blue line *versus* solid yellow green line).

pCa_{50} for P_2 was not significantly different from that for force in either untreated or λPP-treated trabeculae at the short SL (Tables 1 and 2 and Fig. 5*F*), suggesting that in these conditions force is primarily determined by structural changes in the thin filaments. Increasing SL from 1.9 to 2.3 μm increased pCa_{50} for force by ∼0.1 or ∼0.15 pCa units (depending on cTnI and cMyBP-C phosphorylation levels) but the corresponding pCa_{50} changes for P_2 were always smaller (0.05–0.08, about half of the respective force values), regardless of the conditions (Tables 1 and 2 and Fig. 5*F*). This was the case even when reconstitution efficiency was increased from 35% to 50% to ∼80% using an overnight exchange protocol (Fig. S8).

cTnI bisphosphorylation did not have a significant effect on pCa_{50} or ΔpCa_{50} for P_2 in either untreated or λPP-treated trabeculae (Table 2). Back-phosphorylation with PKA significantly increased ΔpCa_{50} for force in trabeculae exchanged with cTn-2P but the PKA-mediated increase in ΔpCa_{50} for P_2 was not statistically significant (Tables 1 and 2 and Fig. 5*F*).

n_H for P_2 was generally less than that for force and in all cases decreased at longer SL (Table 2 and Fig. S9). In untreated trabeculae, increasing cTnI bisphosphorylation decreased cooperativity at the long SL, but in λPP-treated trabeculae, cTn-2P exchange had a bigger effect on n_H for force than on that for P_2 (Fig. S9), similar to the result for pCa_{50}.

N-terminal domains of cMyBP-C bind cardiac troponin in a calcium- and phosphorylation-sensitive manner

MyBP-C has been previously suggested to form interfilament links in resting skeletal muscle (56, 57), and N-terminal domains of cardiac cMyBP-C (NcMyBP-C) have been shown to bind to and modulate the regulatory state of cardiac thin filaments both *in vitro* and *in situ* (47, 58). Moreover, cMyBP-C and cTnI are both PKA targets and together mediate the effect of PKA on LDA. The binding sites for the C0 and C1 cMyBP-C domains on actin are close enough to the C-terminal regions of troponin I to be affected by allosteric rearrangements downstream of PKA phosphorylation (Fig. S10) (59).

We also considered the possibility of a direct interaction between troponin and NcMyBP-C.

To test the hypothesis that the N-terminal domains of cMyBP-C may bind to troponin in heart muscle, we used microscale thermophoresis (MST) to characterize binding between Alexa647-labeled rat cardiac troponin complexes (either cTn-0P or cTn-2P) and N-terminal fragments of rat cMyBP-C encompassing domains C0, C1, m-motif, and C2 (cC0C2), which were either nonphosphorylated (cC0C2-0P) or trisphosphorylated by PKA (cC0C2-3P) (Fig. 6). We found that nonphosphorylated cC0C2 binds both nonphosphorylated cardiac troponin and bisphosphorylated cardiac troponin with an estimated K_D of ∼20 μmol/l in the presence of either low concentrations of Ca^{2+} (pCa 7.4) or saturating calcium (pCa 3.0) (Fig. 6, *A* and *B* inset bar plots). These values are close to previously reported dissociation constants for cC0C2 (C0C1mC2) and cC1C2 (C1mC2) for actin and isolated cardiac native thin filaments. cC0C2 was found to bind actin with a K_D of ∼14 μmol/l (60), and two different studies reported cC1C2 binding native thin filaments with a K_D of ∼10 to 20 μmol/l independent of calcium concentration (60, 61). At low [Ca^{2+}], trisphosphorylation of cC0C2 by PKA reduced its affinity for both nonphosphorylated and bisphosphorylated cTn complex by a factor of two, as indicated by an increase in K_D to ∼40 μmol/l (Fig. 6*A*). The effect of phosphorylation on the cC0C2-cTn interaction was modified in the presence of saturating calcium, which decreased the affinity of PKA-phosphorylated cC0C2 to nonphosphorylated cTn (K_D ∼67 μmol/l) (Fig. 6*B*). Calcium further weakened the interaction between cTn-2P and cC0C2-3P (K_D of ∼141 μmol/l)

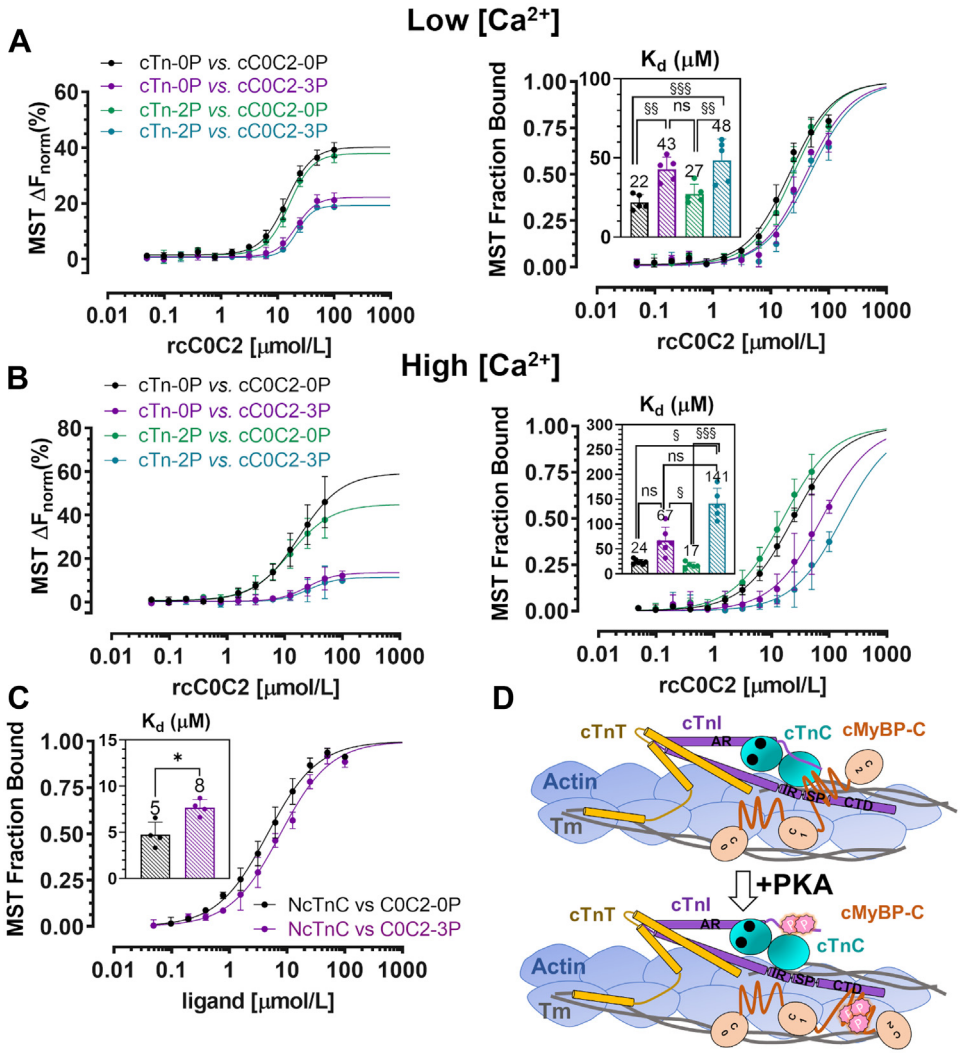

Figure 6. cMyBP-C binds cTn in a cTnI-phosphorylation and calcium-dependent manner. *A*, microscale thermophoresis (MST) curves for nonphosphorylated C0C2 (C0C2-0P) and PKA trisphosphorylated C0C2 (C0C2-3P) binding to nonphosphorylated (cTn-0P) and cTnI bisphosphorylated cTn (cTn-2P) at low Ca^{2+} concentrations (∼pCa 7.4). Left ΔF_{norm} (%): the MST signal change is expressed as the percentage change of the normalized fluorescence (ΔF_{norm}), whereby F_{norm} is defined as F_1/F_0 (fluorescence values before F_0 and after F_1 infrared laser activation) and the baseline F_{norm} (the mean F_{norm} of the unbound target) is subtracted from all data points of the same curve. Right normalized binding: the fraction bound is plotted against ligand concentration, whereby all ΔF_{norm} values of a curve are divided by the curve amplitude, resulting in normalized fraction bound. Inset bar plot of the dissociation constants (K_D). *B*, same as in (*A*), except at high Ca^{2+} concentrations (pCa 3.0). *C*, normalized MST-binding curves for C0C2 (*black*) and C0C2-3P (*purple*) titrated against Alexa647-labeled NcTnC. *D*, hypothetical model of the phosphorylation-dependent interaction of NcMyBP-C with cardiac troponin. Please see text for details. Means ± SD, n = 3 to 5. Statistical significance of differences was assessed with one-way ANOVA, followed by Tukey's post hoc test (*A*) and Kruskal–Wallis test on ranks, followed by Dunn's (*B*) $^{\S}p < 0.05$, $^{\S\S}p < 0.01$, $^{\S\S\S}p < 0.001$. *C*, two-tailed unpaired *t* test $^{*}p < 0.05$.

(Fig. S11). Because the interaction between cTn and NcMyBP-C was sensitive to calcium, we hypothesized that C0C2 might directly bind to NcTnC, which contains the regulatory calcium-binding site and also forms electrostatic interactions with the N-terminal extension of cTnI, carrying the PKA phospho-sites (62). In agreement with this hypothesis, unphosphorylated C0C2 binds NcTnC with an estimated K_D of ∼5 μmol/l at saturating calcium (pCa 3.0), and phosphorylation of C0C2 (C0C2-3P) slightly increased the K_D to ∼8 μmol/l (Fig. 6*C*). Taken together, these results suggest that NcMyBP-C might affect the activation of the thin filament *via* direct interaction with NcTnC, thereby modulating the calcium-dependent activation of the troponin complex (Fig. 6*D*).

Discussion

Signaling through the β_1-adrenoreceptor is paramount for regulating heart structure and function. Most of the physiological effects (chronotropic, inotropic, and lusitropic) are achieved *via* activation of the cAMP-dependent PKA, which phosphorylates several key proteins inside the heart cell, including troponin I. Phosphorylation at both residues Ser22 and Ser23 has been widely regarded as a prerequisite for myofilament Ca^{2+} desensitization, which is a determinant of cardiac relaxation (lusitropy) (30, 63, 64). The underlying mechanism is understood to involve a shift in the equilibrium of NcTnC toward its closed state and a faster rate of calcium dissociation (38, 65, 66). This view is based on studies using different strategies to manipulate or mimic different levels of phosphorylation of troponin I. The most prominent ones are transgenics or protein replacement with cTnI carrying Ser/Ala substitutions, cTnI Ser/Asp substitutions, or troponin I lacking the phosphorylatable N terminus, dephosphorylation using a phosphatase *versus* upphosphorylation using PKA and the application of propranolol *versus* isoprenaline.

In the present study, we replaced endogenous cTnI by either nonphosphorylated or genuinely Ser22/23 bisphosphorylated cTnI to alter the level of cTnI phosphorylation in demembranated trabeculae. We combined this strategy with manipulation of the phosphorylation state of cMyBP-C by λPP and PKA treatment, which allowed us to look at the interaction between cTnI and cMyBP-C phosphorylation. The phosphorylation level of troponin I was measured directly in individual trabeculae after the experiments using Phos-tag-SDS-PAGE and Western blotting against cTnI, which is a key advantage over previous studies, where this was done in time-matched tissue samples. In addition, we demonstrated that our troponin exchange method did not change the phosphorylation status of other major sarcomeric proteins. While the reconstitution protocol itself can alter the contractile response of trabeculae, all groups were subjected to the same treatment, so any functional differences measured between cTn-0P and cTn-2P trabeculae are unlikely to be due to the exchange method. We were therefore able to specifically correlate cTnI bisphosphorylation level with Ca^{2+} sensitivity and LDA in either a low or high cMyBP-C phosphorylation background. This scenario, where the phosphorylation level of one PKA target is varied independently of that of other PKA targets, may not be encountered in the healthy heart, but the results shed light on the mechanism by which PKA modulates heart function at the myofilament level. Contrary to the generally accepted dogma about desensitization, increasing cTnI bisphosphorylation at high levels of cMyBP-C phosphorylation increases calcium sensitivity and decreases cooperativity at long SL. When cMyBP-C was dephosphorylated, these effects were apparent even at short SL and could be detrimental to normal heart muscle function. Therefore, our results have important implications for the diseased heart, where these phosphorylation changes or their consequent functional effects may be uncoupled due to inherited mutations or haploinsufficiency (67, 68).

While others have also observed that increased cTnI phosphorylation did not always produce a rightward shift in the force-calcium relation at short SL (69), most studies reported a reduction in Ca^{2+} sensitivity at both short and long SLs after PKA treatment (15, 70). This discrepancy with the present results may be related to crosstalk with other PKA targets and myofilament phospho-sites, difficulties in separating the effects of monophosphorylation and bisphosphorylation of TnI at Ser22 and 23, species differences, heterologous experimental systems, and the use of phosphomimetics and phosphoablation.

Sarcomeric protein phosphorylation patterns may also be related to the different protocols used in these studies. cTnI phosphorylation is not the sole determinant of myofilament Ca^{2+} sensitivity, which is impacted by phosphorylation background (71). Due to technical difficulties associated with independent modulation of protein phosphorylation levels, many previous studies did not isolate the effects of genuinely phosphorylated cTnI and cMyBP-C. cMyBP-C N-terminal regions have been shown to sensitize the myofilaments to calcium through interactions with actin and tropomyosin and by shifting the position of tropomyosin to favor crossbridge binding (58, 59, 72). PKA phosphorylation of serine residues in the m-domain of cMyBP-C abolishes the activating effect on the thin filament and this inhibition is most apparent for trisphosphorylated N-terminal domains (61). There remains a significant gap of knowledge in the integrated function of genuine multisite phosphorylation of cTnI and cMyBP-C, which future research should address.

"Basal" phosphorylation of myofilament proteins results from sympathetic stimulation before the animal's death but also from residual kinase activity during preparation of the muscle samples. To quantify cTnI phosphorylation, older studies relied on measuring the incorporation of ^{32}P, the relative band intensity from phospho-stains and a phospho-specific antibody against Ser22/23, which is now known to crossreact with monophosphorylated cTnI (37). These methods cannot distinguish between monophosphorylation and bisphosphorylation at Ser22/23. There were early hints that monophosphorylated cTnI might significantly decrease Ca^{2+} sensitivity in skinned muscle preparations (64, 65), and a more recent report described a substantial Ca^{2+}-desensitizing effect of monophosphorylation at Ser23 by PKD when basal

phosphorylation had been abolished by treatment with λPP (37). Moreover, beside PKD, cMLCK has been shown to also phosphorylate Ser23 of cTnI, confirming the functional importance of monophosphorylation (43) and raising further questions about the role of cTnI Ser22/23 bisphosphorylation, which we aimed to address.

Phospho-ablation and phosphomimetics have been used in some previous studies in an attempt to circumvent the problems of basal phosphorylation and multiple kinase/phosphatase targets (38, 39). In one study (38), the endogenous cTnI was extracted from skinned porcine heart muscle, which was then reconstituted with recombinantly generated mouse WT or nonphosphorylatable cTnI (Ser22Ala, Ser23Ala, or Ser22-Ala/Ser23Ala). In that study, *in situ* treatment of skinned cardiac muscle with the catalytic subunit of PKA did not reduce Ca^{2+} sensitivity in the presence of the single alanine cTnI mutants. Only the WT mouse cTnI containing both serines produced the characteristic Ca^{2+} desensitization upon PKA phosphorylation. However, the heterologous protocol with mouse proteins in porcine tissue experiments may complicate the interpretation. There are numerous amino acid mismatches between mouse and porcine cTnI, spread across the entire protein sequence. When cardiac troponin subunits from the same species were used in a homologous experimental system (rat proteins in rat cardiac papillary fibers), double alanine and double aspartate substitutions at Ser22 and Ser23 of cTnI had independent effects, unrelated to PKA, increasing cooperativity and depressing Ca^{2+}-activated maximal tension and ATPase activity (73). Therefore, introducing entirely "silent" phosphomimetic mutations at potential "structurally sensitive sites" may not be always possible (74).

Another study systematically determined the impact of all four combinations of alanine and aspartate substitutions at Ser22/Ser23 in human cardiomyocytes (39). Again, in contrast to the present results, the authors concluded that phosphorylation of both PKA sites was required to reduce myofilament Ca^{2+} sensitivity. That study differs from ours in both the preparation and the use of serine-to-aspartate substitutions. Aspartates are structurally distinct from phosphoserines (75). They differ in size and shape of the side chains and hydrated shell, the charge and the surrounding chemical environment, which could affect intramolecular and intermolecular hydrogen bonds, salt bridges, and ionic interactions. Moreover, we previously showed that aspartates are not functional substitutes for phosphoserines in cMyBP-C with different impact on thin filament regulation (35).

Muscle preparations from transgenic mice overexpressing the nonphosphorylatable, slow skeletal isoform of TnI or Ser22/23 phospho-ablated cardiac TnI had reduced desensitization in response to PKA, supporting the hypothesis that Ser22/23 cTnI phosphorylation reduces Ca^{2+} sensitivity (30, 76). However, replacing the cardiac troponin I isoform by the slow skeletal isoform has similar limitations as the use of heterologous proteins or amino acid substitutions. We conclude that findings from these types of transgenic study need to be considered more critically and verified by alternative methods.

We used dephosphorylation by a protein phosphatase and back-phosphorylation with PKA to control myofibrillar protein phosphorylation levels, an approach that has also been used in previous studies (37, 69). A negative correlation has been demonstrated between cTnI phosphorylation and Ca^{2+} sensitivity when troponin exchange, phosphatase, and PKA treatment were used to alter cTnI phosphorylation levels in donor human heart myofibrils and *in vitro* motility assays (69, 77). *In vitro* motility assays often use heterologous proteins, lack key sarcomeric components, and cannot fully reproduce the functional response of a muscle cell. Moreover, cTnI is not the only target of λPP and PKA, which complicates the relationship between Ca^{2+} sensitivity and cTnI phosphorylation. Although λPP and PKA had the same limitations in our study, we did not use them to control cTnI phosphorylation level, which was modulated separately and specifically *via* troponin exchange. In our study, λPP and PKA were used to control the phosphorylation level of other myofilament targets in order to determine the context-specific effects of cTnI bisphosphorylation. We propose that increasing bisphosphorylation only increases calcium sensitivity when cMyBP-C phosphorylation is not increased simultaneously. When both cTnI and cMyBP-C are phosphorylated by PKA, there is a substantial body of evidence pointing to a desensitizing effect of PKA treatment on the myofilament response to calcium (78–80).

Replacement of the endogenous troponin in human cardiomyocytes with either nonphosphorylated human cardiac troponin (in donor samples) or bisphosphorylated human cardiac troponin (in failing tissue) produced mixed populations of nonphosphorylated, monophosphorylated, and bisphosphorylated cTnI, consistent with the present results (71). The overall effect of decreasing the proportion of bisphosphorylated cTnI in donor cardiomyocytes was an increase in calcium sensitivity but the confounding effect of decreasing the proportion of monophosphorylated cTnI was not considered. We were also not able to eliminate the proportion of monophosphorylated cTnI, probably due to residual kinase and phosphatase activities and incomplete troponin exchange. However, the levels of monophosphorylation in our study were similar (20%–30%) in the cTn-0P and cTn-2P groups and therefore unlikely to be responsible for the functional effects. Both donor and failing heart groups with similar levels of cTnI monophosphorylation and higher levels of cTnI bisphosphorylation exhibited a slight leftward shift of the force-pCa relation, albeit not statistically significant. The difference from our results may also stem from species-specific differences (human *versus* rat). When skinned cardiac rat myocytes were exchanged with nonphosphorylated rat troponin, PKA treatment increased Ca^{2+} sensitivity (81), as in the present study.

Although cTn-2P exchange had a significant effect on the pCa_{50} of force at long SL in untreated trabeculae, the effect on pCa_{50} of the structural change reported by the troponin probe was small and not statistically significant. Similarly, in λPP-treated trabeculae, cTn-2P exchange influenced pCa_{50} of force but not that of P_2. This could be because the probe is on

troponin C and not on troponin I, but it could also be a fundamental feature of the PKA mechanism and dual filament regulation. PKA phosphorylation of troponin I may be communicated to the thick filament to increase its activation state and LDA. Therefore, force would be a better indicator for such a mechanism because it depends on the activation states of both filaments.

In addition to the effects on Ca^{2+} sensitivity described before, increasing the proportion of bisphosphorylated cTnI also affected the cooperativity of the force-pCa relations as described by the Hill coefficient n_H. In trabeculae that had been nonspecifically dephosphorylated with λPP, exchange with cTn-2P reduced n_H for force at both the short and long SLs in comparison with the cTn-0P group. Back-phosphorylation with PKA increased n_H for force to the levels seen in the λPP-treated cTn-0P group, indicating that the effect is related to the mismatched phosphorylation levels of cTnI and other sarcomeric PKA targets. This result shows that cTnI bisphosphorylation can have a detrimental impact on the force-calcium response when it is not coordinated with the phosphorylation status and action of its partners.

The activation of thin and thick filaments is intrinsically cooperative, and both filaments are likely to influence the steepness of the force-calcium relation as measured by n_H (6, 48). Troponin–tropomyosin interactions facilitate the spread of activation between adjacent regulatory units along the thin filament (2), whereas thick filament cooperativity may rely on the intermolecular myosin head–head interactions, which could propagate structural changes along its length (6, 82). Links between thick and thin filaments enhance cooperativity through interfilament signaling ensuring that activation is coordinated between the filament systems (83, 84). Therefore, interventions that affect interfilament communication by changing crossbridge states or cMyBP-C N-terminal interactions would be expected to alter the level of cooperativity (85, 86). We hypothesize that the mismatched phosphorylation states of cTnI and cMyBP-C impair interfilament signaling, leading to a reduction in the Hill coefficient for force. The impact of cTnI bisphosphorylation on Ca^{2+} sensitivity and cooperativity in the absence of synchronized changes in cMyBP-C phosphorylation implies that the effects of PKA in the healthy heart must be mediated by coordinated changes in the phosphorylation states of both cTnI and cMyBP-C.

PKA treatment of permeabilized muscle preparations has been shown to enhance LDA but the contributions of cTnI and cMyBP-C phosphorylation have not been clearly defined (15). Our experiments show that when cMyBP-C is phosphorylated, incorporation of nonphosphorylated troponin resulted in a lower length-dependent shift in calcium sensitivity. The relative percentage of bisphosphorylated cTnI positively correlated with ΔpCa_{50} associated with LDA. When cMyBP-C phosphorylation level was reduced, however, cTnI bisphosphorylation at Ser22 and Ser23 did not augment ΔpCa_{50}. Moreover, in λPP-dephosphorylated trabeculae, the relative percentage of bisphosphorylated cTnI no longer correlated with ΔpCa_{50}. Back-phosphorylation with PKA restored cMyBP-C phosphorylation levels and increased ΔpCa_{50}, suggesting that cTnI and cMyBP-C work together to upregulate LDA downstream of β-adrenergic signaling.

The conclusion that phosphorylation of cMyBP-C and cTnI enhances LDA through a shared mechanism is consistent with previous studies showing that modifications to just one of those proteins can block the PKA-dependent increase in LDA (46, 87, 88). These findings are based on phosphoablation and KO models, which have inherent limitations as discussed previously. Other studies using phosphomimetics and phosphoablation have been interpreted in terms of independent effects of cTnI and cMyBP-C phosphorylation on LDA (18) or to imply that cMyBP-C is mainly responsible for the response to β-adrenergic stimulation (27), which highlights the need for more physiological experimental systems.

Our results are consistent with a molecular model in which PKA phosphorylation acts through both cTn and cMyBP-C on calcium sensitivity, cooperativity, and LDA in isolated myocardium. A direct interaction with troponin, the calcium sensor on the thin filament and subject to phosphorylation by the same kinase, might explain the coordinated responses of these two proteins to PKA phosphorylation.

Our MST data show that C0C2 can directly bind to the cardiac troponin core-complex *in vitro*. Such an interaction has already been reported (89) but here we provide context to its regulation by phosphorylation and calcium. N-terminal domains of cMyBP-C have been shown to diffuse along isolated thin filaments, scanning the filament for regulatory binding sites (83), which could be either actin sites or troponin based on their availability. In addition, cryo-EM structures show that there is an overlap between troponin, myosin, and C0C1 binding sites on actin, so it is possible that phosphorylation, calcium, and ligand competition determine their occupancy (2, 59, 90).

Although binding of NcMyBP-C to the thin filament is generally associated with an activating effect and an increase in its calcium sensitivity, the functional consequences of NcMyBP-C–cTn interactions could be different. NcMyBP-C also binds to NcTnC *in vitro*, which could either promote or interfere with cTnI switch peptide binding to NcTnC. This hypothesis could be tested in future experiments.

In the thick filament, C-zone cMyBP-C is organized into nine stripes each containing three molecules, giving a total of 27 cMyBP-Cs per thick filament. In contrast, in the same region, there are about ∼40 available troponin molecules per thick filament and seven times more actins. Considering the similar affinities of NcMyBP-C for actin and troponin and their stoichiometries, cMyBP-C might only bind a small fraction of cardiac troponins. However, only a fraction of thin filament regulatory units is activated during peak systole (7) and the activation signal is likely transmitted between troponins *via* structural changes in the tropomyosin chain. Moreover, the local effective concentrations of NcMyBP-C and cardiac troponin are in the high micromolar range (61), which makes dissociation constants in the low micromolar range functionally significant.

Tris-phosphorylation of cMyBP-C not only weakens the interaction between NcMyBP-C and cardiac myosin, leading

to a redistribution of the majority of NcMyBP-C toward the thin filament, but also weakens the interaction of NcMyBP-C with bisphosphorylated cardiac troponin. In agreement, phosphorylation of isolated NcMyBP-C reduces binding (B_{max}) to isolated thin filaments (61). It follows that during these conditions NcMyBP-C primarily occupies actin-binding sites on the thin filament because of the aforementioned stoichiometry considerations and the lower affinity for cTn-2P compared to actin.

This new phospho-regulated interaction between troponin and cMyBP-C gives an insight into the mechanism of their functional integration downstream of PKA. However, the molecular details of cMyBP-C interacting with cardiac myosin and thin filaments are currently unknown. Therefore, our findings should be treated as a starting point for further investigations.

There are several limitations in our study. λPP treatment is not 100% efficient and is nonspecific, affecting multiple sarcomeric components in trabeculae. We have previously shown that incubation with λPP increases the calcium sensitivity and decreases the cooperativity of the force-calcium relation but has no effect on the maximal calcium activated force of rat ventricular trabeculae (43). We assessed trabeculae and cardiac myofibril samples using ProQ/SYPRO to check which proteins were differentially modified by λPP and PKA (Figs. 1 and S6). In our preparation, the cardiac regulatory light chain of myosin (cRLC) was not phosphorylated (see Fig. S6) (91), a result which may differ from that of other studies due to different animal strains and protocols. Hence, cRLC phosphorylation was not a factor in our experiments. In contrast to λPP, PKA is a specific enzyme and only increases the phosphorylation of its preferred targets including cMyBP-C and cTnI. The additional λPP, PKA control group, in combination with the specific cTnI exchange allowed us to distinguish between nonspecific and specific functional effects.

While we did not measure the changes in titin phosphorylation, we were able to compare passive tension before and after PKA treatment. PKA phosphorylation of titin reduces passive tension (92, 93), which we observed in PKA back-phosphorylated trabeculae that were pretreated with λPP (Table 1). We did not have the tools to study the effects of titin phosphorylation independently, but we expect it to change in the same direction as that of cMyBP-C in the aforementioned experiments. We cannot exclude the possibility that titin phosphorylation contributes to the changes observed alongside cMyBP-C, and a coordinated interplay between all three myofilament PKA targets (cTnI, cMyBP-C, and titin) may control the response to PKA *in vivo*.

Another limitation of our study is that we examined steady state parameters in Ca^{2+} titrations. Although calcium sensitivities measured in steady-state experiments with permeabilized muscle preparations do not reproduce the dynamic behavior of the heart, they can be useful indicators for trends toward either increased or decreased relaxation (94). By looking at the structure and force parameters at the physiological diastolic (∼pCa 7.0) and systolic calcium levels (∼pCa 6.0) (54, 95), we can enhance our understanding of the PKA mechanism in simple steady-state conditions, so that we can later address more complex processes on the timescale of the heartbeat. The kinetics of heart muscle contraction and relaxation are impacted by many other sarcomeric and non-sarcomeric factors, which are poorly understood.

We did not use a sarcomere clamp method, so shortening in the central segment of the trabeculae during activation may have led to underestimation of the length-dependent changes in the measured parameters. However, we do not expect this to fundamentally change our results or conclusions, since the same limitation applied to all protocols. The temperature was lower (21–23 °C) than physiological because our protocols were optimized for modulation of cTnI phosphorylation. It is difficult to increase the temperature to physiological values without compromising cTnI phosphorylation status or inflicting additional damage to the λPP-treated trabeculae.

In summary, the functional effects of PKA phosphorylation in demembranated trabeculae are highly coordinated between its major targets cTnI and cMyBP-C. This level of coordination might be enabled by direct interactions and competition for actin-binding sites on thin filament, subject to regulation by PKA. When cTnI bisphosphorylation is elevated at low levels of cMyBP-C phosphorylation, trabeculae show higher calcium sensitivity, depressed length-dependent shift in calcium sensitivity, and depressed cooperativity. This could have pathological consequences for the heart, particularly in disease settings where cMyBP-C phosphorylation or phospho-regulated function is impaired.

Experimental procedures

Protein production and PKA phosphorylation

The rat cardiac troponin subunits were cloned, expressed, and purified separately. The whole troponin complex was reconstituted as previously described (43). As required, the complex was incubated with the catalytic subunit of PKA (Calbiochem, 539576) at a molar ratio ∼1:100 (PKA:cTnI) overnight at 30 °C in a buffer containing 50 mmol/l Tris–HCl pH 8, 100 mmol/l NaCl, 5 mmol/l $MgCl_2$, 1 mmol/l $CaCl_2$, 5 mmol/l ATP, and 1 mmol/l DTT. Subsequent mass spectrometric and Phos-tag immunoblot analysis showed that only Ser 22 and Ser 23 on cTnI were phosphorylated with ∼100% efficiency (Fig. S3). Cardiac troponin was purified by running it through a Resource-Q column. The final concentrated product was subjected to further analysis by HPLC, electrospray ionization-mass spectrometry, and size-exclusion–multiangle light scattering (Figs. S4 and S5). The C0C2 fragments from rat cardiac MyBP-C were produced using the same methods described for C1mC2 fragments (47, 61).

Trabeculae preparation

All animals were treated in accordance with the guidelines approved by the UK Animal Scientific procedures Act (1986) and European Union Directive 2010/63/EU. Male Wistar rats (200–250 g) were sacrificed by cervical dislocation without the use of anesthetics (Schedule 1 procedure in accordance with UK Animal Scientific Procedure Act, 1986). Right ventricular

trabeculae were dissected as previously described (48) but the dissection solution contained 50 mmol/l butanedionemonoxime (BDM) and was kept ice-cold to prevent tissue damage and reduce hyperphosphorylation of myofilament proteins during the preparation. Calpeptin (25 μmol/l, Merck Milipore, 03-34-0051-5MG) was also supplemented to inhibit calpain activity during permeabilization in 1% Triton X-100. Demembranated trabeculae were stored in relaxing solution (96) containing 50% (v/v) glycerol, 1% (v/v) protease inhibitor cocktail (Sigma–Aldrich, P8340), and kinase inhibitors H-89 (50 μmol/l, Abcam, ab143787) and H7 (20 μmol/L, Abcam, ab142308) at −20 °C for 1 week. Trabeculae to be dephosphorylated with lambda protein phosphatase (λPP) were preserved in 50% (v/v) glycerol storage relaxing buffer without kinase or phosphatase inhibitors. After λPP treatment, trabeculae were kept in the storage solution with all the aforementioned inhibitors including 1% (v/v) phosphatase inhibitor cocktail 3 (Sigma–Aldrich, P0044).

Lambda phosphatase treatment and PKA back-phosphorylation

Trabeculae and time-matched tissue samples to be treated with λPP were split into three groups: λPP-treatment and nonphosphorylated cTn exchange (λPP, cTn-0P), λPP-treatment and bis-phosphorylated cTn exchange (λPP, cTn-2P), and finally λPP-treatment followed by PKA back-phosphorylation and cTn-2P exchange (λPP, PKA, cTn-2P). For λPP dephosphorylation, the trabeculae were incubated 2 h at 20 °C in a buffer with the same composition as relaxing buffer (96) excluding K_2EGTA with additional 50 mmol/l BDM, 13 mmol/l $MnCl_2$, and 2000 U/ml λPP (New England BioLabs, P0753). After the λPP treatment, some tissue samples were harvested for gels by washing them two times in PBS (1× PBS) and boiling in denaturing 1× sample buffer for 10 min (45 mmol/l Tris–HCl pH 6.8, 1% SDS, 10% glycerol, 1% β-mercaptoethanol, 0.01% bromphenol blue). The third group of trabeculae and muscles were washed in PKA buffer (relaxing solution supplemented with 50 mmol/l BDM, 1% (v/v) protease inhibitor cocktail, 25 μmol/l calpeptin, and 1% (v/v) phosphatase inhibitor cocktail 3), followed by back-phosphorylation in PKA buffer containing 20 U/μl of the kinase for 2 h at 20 °C.

Troponin exchange

The trabeculae were exchanged with rat cTn (either 0P or 2P) by bathing them overnight at 4 °C in relaxing solution containing 1.5 mg/ml troponin, 50 mmol/l BDM, 1% (v/v) protease inhibitor cocktail, and kinase inhibitors H-89 and H7 (50 μmol/l and 20 μmol/l, respectively). The exchange solution for λPP dephosphorylated trabeculae also contained 1% (v/v) phosphatase inhibitor cocktail 3 and calpeptin (25 μmol/l). The 2P cTn exchange solution for λPP dephosphorylated and PKA back-phosphorylated trabeculae contained 20 U/μl PKA, 50 mmol/l BDM, 1% (v/v) protease inhibitor cocktail, 1% (v/v) phosphatase inhibitor cocktail 3, and calpeptin (25 μmol/l). On the following morning, the troponin-reconstituted trabeculae were exchanged with BR-cTnC-E in a second step for 2.5 h at 4 °C. The exchange solution contained 0.5 mg/ml BR-cTnC-E, 50 mmol/l BDM, and the same inhibitors as in the previous troponin solution. Whole troponin reconstitution was previously assessed as ∼80% (43). BR-cTnC-E exchange efficiency is shown in Fig. S2, and the method was described in an earlier study (3).

Determination of cTnI phosphorylation level

After experiments, trabeculae were washed two times briefly in 1× PBS and dismounted from the experimental setup. Trabeculae and time-matched muscles were dissolved in 1× Laemmli sample buffer as previously described. Protein samples were run on 10% (v/v) acrylamide mini-PROTEAN or CRITERION (Bio-Rad) Phos-tag-SDS-PAGE gels (containing 50 μmol/l Phos-tag-reagent and 100 μmol/l $MnCl_2$) at constant current of 20 mA per gel. The Western blot protocol was described earlier with some modifications (43). The proteins were blotted onto polyvinylidene difluoride membranes for 1 h at 1 mA/cm^2 using a Trans-Blot SD Semi-Dry Electrophoretic Transfer Cell (Bio-Rad). The membranes were blocked overnight in Tris-buffered saline containing 0.05% (v/v) Tween 20 (TBS-T) and 5% (w/v) semiskimmed milk powder and probed with the following mouse monoclonal primary antibodies in TBS-T and 1% (w/v) semiskimmed milk powder for 2 h at 4 °C (working dilution, source, catalog #): mouse anti-cTnI antibody [MF4] (1: 10,000, HyTest, 4T21) and mouse anti-cTnI antibody [84] (1: 5,000, HyTest, 4T21). Anti-cTnI [MF4] detects an epitope at the C terminus of cTnI WRKNIDA (aa 190–196 in the human sequence and 191–197 in rat cTnI), which is identical in human and rat. In comparison, anti-cTnI [84] binds to residues VTKNITEIAD, part of the coiled coil region (human 117–126 and rat 118–127). The rationale for using both antibodies was to check for any major differences in phosphorylation levels resulting from C-terminally degraded cTnI. For immunoblotting using the polyclonal antibodies against phospho-cTnI (1:500 in TBS-T and 1% (w/v) bovine serum albumin [BSA], Cell Signaling, 4004) and total cTnI (1:1000 in TBS-T and 1% (w/v) semiskimmed milk powder, Cell Signaling, 4002), the membrane was blocked for 1 h in TBS-T and 5% (w/v) of the corresponding blocking reagent before overnight incubation with the primary antibody at 4 °C. Membranes were agitated for 30 min at 4 °C in the secondary antibody solution: horseradish peroxidase (HRP)–conjugated goat antimouse IgG (1:2000 in TBS-T and 1% (w/v) semiskimmed milk powder, Bio-Rad, 103005) or HRP-conjugated goat anti-rabbit IgG (1:2000 in TBS-T and 1% (w/v) blocking reagent, Bio-Rad, 403005) as appropriate.

For phosphostaining, samples were run on either 10% (v/v) acrylamide SDS-PAGE gels or 4% to 20% (v/v) gradient gels (Bio-Rad). The gels were stained with Pro-Q Diamond phosphoprotein stain and SYPRO Ruby total protein stain according to the manufacturer's instructions (Life Technologies).

Determination of cMyBP-C phosphorylation level

CMFs were prepared as previously described (85). The CMF pellet weights were measured after the last centrifugation step

to determine the concentration in CMF buffer. The pellets were resuspended in CMF buffer and 50% (v/v) glycerol for storage at −20 °C. Inhibitors were supplemented to all solutions at the same concentrations used for trabeculae. CMFs from each heart were split into three samples each: before treatment (PRE), λPP sample, and λPP/PKA sample. The pellets were washed three times in λPP buffer. CMFs were dephosphorylated using the same conditions as for trabeculae: 20 mg pellet in 1 ml phosphatase buffer containing 2000 U/ml λPP and inhibitors for 2 h at 20 °C. The λPP/PKA samples were washed in relaxing solution before back-phosphorylation for 2 h at 4 °C with 20 U/μl PKA as previously described for trabeculae. SDS-PAGE samples were prepared as before.

For ProQ/SYPRO staining, the samples were run on 10% (v/v) acrylamide gel. For Western blotting against cMyBP-C, the samples were run on a 6% (v/v) acrylamide gel. The transfer buffer contained 5% (v/v) methanol and semidry transfer was performed for 2 h. BSA was used as a blocking agent for the phospho-specific primary antibody against S282 phosphorylated cMyBP-C. Primary incubation took place overnight at 4 °C (1:2,000, ENZO Life Sciences, AL-215-057-R050). The antibody is expected to bind to residues 276 to 288 (G276AGRRTpSDSHEDA288) of cMyBP-C phosphorylated at Ser282. The protocol for secondary antibody incubation and onward was as previously described (HRP-conjugated goat anti-rabbit IgG, 1:2000 dilution, Bio-Rad, 403005). To detect total cMyBP-C, the membrane was stripped using Restore Plus stripping agent (Thermo Scientific). Stripping was done for 45 min at 20 °C according to the provided instructions, followed by a wash and blocking in 5% (w/v) BSA and 1× TBS-T. Total cMyBP-C was detected with anti-cMyBP-C mouse monoclonal IgG [G-7]: 1:2000 for 5 h at 4 °C (Santa Cruz Biotechnology, sc-137237). The secondary antibody was HRP-conjugated goat antimouse IgG (1:2000, Bio-Rad, 103005).

MST

Recombinant troponin complexes (either 0P or 2P) were labeled with Alexa647-NHS (ThermoScientific) at a stoichiometry 1:1 according to the manufacturer's instructions. The reactions were stopped with 50 times molar excess Tris–HCl and cleaned of free dye using a Nap5 column. Dye incorporation efficiency (>80%) was confirmed by HPLC and using the Alexa647 extinction coefficient. For the cTnC N-lobe experiments (NcTnC), NcTnC was labeled with Alexa647-NHS using the same protocol. Recombinant rat cardiac C0C2 fragments (either 0P or PKA phosphorylated 3P) were exchanged in the corresponding MST buffer. The low-Ca^{2+} MST buffer contained 20 mmol/l Mops, pH 7, 1 mmol/l K-EGTA, 100 μmol/l $CaCl_2$, 1 mmol/l $MgCl_2$, 50 mmol/l KCl, 1 mmol/l DTT, 0.05% (v/v) Tween 20. The high-Ca^{2+} MST buffer contained 1 mmol/l $CaCl_2$ in the absence of K-EGTA and $MgCl_2$ and was also used for the NcTnC experiments. Twelve (1:1) dilutions were prepared, producing ligand C0C2 concentrations ranging from 0.0488 μM to 100 μM. The concentration of the Alexa647-labeled cTn was kept constant at 90 nmol/l and the concentration of Alexa647-labeled NcTnC was 50 nmol/l. After 20 min incubation, followed by centrifugation at maximum speed in a table-top centrifuge for 1 min, the samples were loaded into Monolith NT.115 [Premium] Capillaries (NanoTemper Technologies). The troponin complex MST measurements were performed using the Monolith NT.115 [NT.115Pico/NT.LabelFree] (NanoTemper Technologies) at 20% LED power, 40% medium MST power, and 30 °C. The cTnC N-lobe experiments were performed at 20% LED power, 80% MST power, and 30 °C. The same MST-on time was used for comparisons (MO.Affinity Analysis software version 2.2.4, NanoTemper Technologies). The experiment numbers represent independently pipetted measurements.

Fluorescence polarization experiments

From each preparation, trabeculae were split into either two groups (untreated trabeculae) or three groups (λPP-treated trabeculae) to minimize the impact of animal-to-animal variations. Two experiments were performed each day in a randomized order. Polarized fluorescence intensities and force were measured simultaneously as described previously at 20 °C (48). In brief, trabeculae were illuminated from below with laser light polarized either parallel or perpendicular to the trabecular axis. Fluorescence emission from BR-cTnC-E in trabeculae was collected both in line with the illuminating beam and at 90° to both the illuminating beam and the trabecular axis. Each emitted beam was separated into parallel and perpendicular components, from which three independent orientation order parameters were calculated: P_{2d} describing the amplitude of rapid probe wobble on the protein surface and P_2 and P_4 describing the distribution of angles θ between the BR fluorescence dipole and the thin filament axis (97). The order parameter P_2 is linearly related to populations of probe molecules in the muscle cell and takes values between +1 (parallel orientations) and -0.5 (perpendicular orientations).

The SL was measured by laser diffraction in relaxing solution and initial SL was adjusted to 1.9 μm. The composition of the experimental solutions was previously described (96). Each activation was preceded by a 2 min incubation in preactivating solution. Solutions with varying free [Ca^{2+}] were prepared by mixing relaxing and activating solutions according to calculations using the MAXCHELATOR software (maxchelator.stanford.edu). For experiments in untreated trabeculae, calpeptin and kinase inhibitor H7 were supplemented at the concentrations aforementioned. Additional phosphatase inhibitor cocktail 3 was supplemented to all λPP-treated trabeculae. Trabeculae were activated by switching pCa solutions using a continuous titration protocol to limit damage to the trabeculae. Force was recorded once steady state was established. Trabeculae were relaxed after maximal activation. Trabeculae in which force at maximal [Ca^{2+}] declined by more than 15% were discarded. After the first titration, trabeculae were stretched to SL 2.3 μm in relaxing solution and the titration protocol was repeated.

Data analysis

The force-pCa and P_2-pCa relations were fitted for each trabecula using nonlinear least-squares regression to a modified Hill equation:

$$Y = Y_0 + \frac{(Y_{MAX} - Y_0)}{\left[1 + 10^{n_H(pCa - pCa_{50})}\right]}$$

whereby, n_H is the Hill coefficient, Y_{MAX} is the maximal value, and Y_0 is the minimal value of force or P_2. pCa_{50} indicates the inverse log of the $[Ca^{2+}]$ required for 50% of the total change in Y.

Correlations between cTnI phosphorylation level and Ca^{2+} sensitivity of force or length-dependent changes in force pCa_{50} were evaluated in SigmaPlot (version 14.0). Correlation of these parameters was tested using Pearson analysis. The data were plotted using Prism (version 8.2.1).

Unpaired Student t test was used for comparisons between two groups (untreated trabeculae exchanged with cTn-0P *versus* untreated trabeculae exchanged with cTn-2P) when homoscedasticity and normality assumptions were met. Mann–Whitney Rank Sum Test was used if Shapiro–Wilk normality or Brown–Forsythe equal variance tests failed. Many of the effects due to SL have been previously characterized by us and others and we had clearly defined hypotheses (10, 13, 98). Therefore, instead of using mixed design analysis, paired Student t tests were performed for comparisons between SL 1.9 μm and 2.3 μm. Wilcoxon Signed Rank Test was used for nonparametric comparisons.

Unless otherwise specified, the λPP set of experiments were analyzed using one-way *versus* the λPP-treated group exchanged with cTn-2P in combination with Holm–Sidak post-test, when assumptions of normality and homoscedasticity were satisfied. Alternatively, Kruskal–Wallis one-way analysis on ranks against the λPP-treated cTn-2P group was performed, followed by Dunn's post-test. Within-group analysis between SL 1.9 μm and 2.3 μm was done as previously stated. All data were expressed as mean ± SD, with N referring to the number of animals and n representing the number of muscles. Statistical significance was set at $p < 0.05$.

Data availability

All data are contained within the article and supplemental information. Raw data can be obtained from the corresponding author upon reasonable request.

Supporting information—This article contains supporting information (1, 2, 59, 62, 90).

Acknowledgments—We are grateful to the British Heart Foundation for their financial support. We also thank Dr Andrea Knowles, Professor Metin Avkiran, Professor Brian Sykes and Professor Jonathan Kentish for their help and advice.

Author contributions—I. R. S., T. K., and Y. B. S. methodology; I. R. S. formal analysis; I. R. S. investigation; S. P. and Z. Y. resources; I. R. S., M. I., and T. K. writing–original draft.

Funding and additional information—This study was funded by a senior basic science fellowship awarded to Y. B. S. (FS/15/1/31071) and a basic science intermediate fellowship awarded to T. K. (FS/16/3/31887).

Conflict of interests—The authors declare that they have no conflicts of interest with the contents of this article.

Abbreviations—The abbreviations used are: BSA, bovine serum albumin; BR, bifunctional rhodamine; CMF, cardiac myofibril; HRP, horseradish peroxidase; LDA, length-dependent activation; MST, microscale thermophoresis; SL, sarcomere length; TBS-T, Tris-buffered saline containing 0.05% (v/v) Tween 20.

References

1. Takeda, S., Yamashita, A., Maeda, K., and Maeda, Y. (2003) Structure of the core domain of human cardiac troponin in the Ca(2+)-saturated form. *Nature* **424**, 35–41
2. Yamada, Y., Namba, K., and Fujii, T. (2020) Cardiac muscle thin filament structures reveal calcium regulatory mechanism. *Nat. Commun.* **11**, 153
3. Sevrieva, I., Knowles, A. C., Kampourakis, T., and Sun, Y. B. (2014) Regulatory domain of troponin moves dynamically during activation of cardiac muscle. *J. Mol. Cell Cardiol.* **75**, 181–187
4. Linari, M., Brunello, E., Reconditi, M., Fusi, L., Caremani, M., Narayanan, T., *et al.* (2015) Force generation by skeletal muscle is controlled by mechanosensing in myosin filaments. *Nature* **528**, 276–279
5. Reconditi, M., Caremani, M., Pinzauti, F., Powers, J. D., Narayanan, T., Stienen, G. J., *et al.* (2017) Myosin filament activation in the heart is tuned to the mechanical task. *Proc. Natl. Acad. Sci. U. S. A.* **114**, 3240–3245
6. Kampourakis, T., Sun, Y. B., and Irving, M. (2016) Myosin light chain phosphorylation enhances contraction of heart muscle *via* structural changes in both thick and thin filaments. *Proc. Natl. Acad. Sci. U. S. A.* **113**, E3039–3047
7. Brunello, E., Fusi, L., Ghisleni, A., Park-Holohan, S. J., Ovejero, J. G., Narayanan, T., *et al.* (2020) Myosin filament-based regulation of the dynamics of contraction in heart muscle. *Proc. Natl. Acad. Sci. U. S. A.* **117**, 8177–8186
8. Allen, D. G., and Kentish, J. C. (1985) The cellular basis of the length-tension relation in cardiac muscle. *J. Mol. Cell Cardiol.* **17**, 821–840
9. Sequeira, V., and van der Velden, J. (2015) Historical perspective on heart function: the frank-starling law. *Biophys. Rev.* **7**, 421–447
10. de Tombe, P. P., Mateja, R. D., Tachampa, K., Mou, Y. A., Farman, G. P., and Irving, T. C. (2010) Myofilament length dependent activation. *J. Mol. Cell Cardiol.* **48**, 851–858
11. Piazzesi, G., Caremani, M., Linari, M., Reconditi, M., and Lombardi, V. (2018) Thick filament mechano-sensing in skeletal and cardiac muscles: a common mechanism able to adapt the energetic cost of the contraction to the task. *Front. Physiol.* **9**, 736
12. Li, K. L., Rieck, D., Solaro, R. J., and Dong, W. (2014) *In situ* time-resolved FRET reveals effects of sarcomere length on cardiac thin-filament activation. *Biophys. J.* **107**, 682–693
13. Zhang, X., Kampourakis, T., Yan, Z., Sevrieva, I., Irving, M., and Sun, Y. B. (2017) Distinct contributions of the thin and thick filaments to length-dependent activation in heart muscle. *Elife* **6**, e24081
14. Ait-Mou, Y., Hsu, K., Farman, G. P., Kumar, M., Greaser, M. L., Irving, T. C., *et al.* (2016) Titin strain contributes to the Frank-Starling law of the heart by structural rearrangements of both thin- and thick-filament proteins. *Proc. Natl. Acad. Sci. U. S. A.* **113**, 2306–2311
15. Konhilas, J. P., Irving, T. C., Wolska, B. M., Jweied, E. E., Martin, A. F., Solaro, R. J., *et al.* (2003) Troponin I in the murine myocardium: influence

on length-dependent activation and interfilament spacing. *J. Physiol.* **547**, 951–961
16. Sequeira, V., and van der Velden, J. (2017) The frank-starling law: a jigsaw of titin proportions. *Biophys. Rev.* **9**, 259–267
17. Hanft, L. M., Biesiadecki, B. J., and McDonald, K. S. (2013) Length dependence of striated muscle force generation is controlled by phosphorylation of cTnI at serines 23/24. *J. Physiol.* **591**, 4535–4547
18. Kumar, M., Govindan, S., Zhang, M., Khairallah, R. J., Martin, J. L., Sadayappan, S., *et al.* (2015) Cardiac myosin-binding protein C and troponin-I phosphorylation independently modulate myofilament length-dependent activation. *J. Biol. Chem.* **290**, 29241–29249
19. Hidalgo, C., and Granzier, H. (2013) Tuning the molecular giant titin through phosphorylation: role in health and disease. *Trends Cardiovasc. Med.* **23**, 165–171
20. Pulcastro, H. C., Awinda, P. O., Breithaupt, J. J., and Tanner, B. C. (2016) Effects of myosin light chain phosphorylation on length-dependent myosin kinetics in skinned rat myocardium. *Arch. Biochem. Biophys.* **601**, 56–68
21. Sequeira, V., Wijnker, P. J., Nijenkamp, L. L., Kuster, D. W., Najafi, A., Witjas-Paalberends, E. R., *et al.* (2013) Perturbed length-dependent activation in human hypertrophic cardiomyopathy with missense sarcomeric gene mutations. *Circ. Res.* **112**, 1491–1505
22. Najafi, A., Sequeira, V., Kuster, D. W., and van der Velden, J. (2016) beta-adrenergic receptor signalling and its functional consequences in the diseased heart. *Eur. J. Clin. Invest.* **46**, 362–374
23. Hanft, L. M., and McDonald, K. S. (2009) Sarcomere length dependence of power output is increased after PKA treatment in rat cardiac myocytes. *Am. J. Physiol. Heart Circ. Physiol.* **296**, H1524–1531
24. Bers, D. M. (2002) Cardiac excitation-contraction coupling. *Nature* **415**, 198–205
25. Solaro, R. J. (2008) Multiplex kinase signaling modifies cardiac function at the level of sarcomeric proteins. *J. Biol. Chem.* **283**, 26829–26833
26. Fukuda, N., and Granzier, H. L. (2005) Titin/connectin-based modulation of the Frank-Starling mechanism of the heart. *J. Muscle Res. Cell Motil.* **26**, 319–323
27. Gresham, K. S., and Stelzer, J. E. (2016) The contributions of cardiac myosin binding protein C and troponin I phosphorylation to beta-adrenergic enhancement of *in vivo* cardiac function. *J. Physiol.* **594**, 669–686
28. Solaro, R. J., Moir, A. J., and Perry, S. V. (1976) Phosphorylation of troponin I and the inotropic effect of adrenaline in the perfused rabbit heart. *Nature* **262**, 615–617
29. Wijnker, P. J., Murphy, A. M., Stienen, G. J., and van der Velden, J. (2014) Troponin I phosphorylation in human myocardium in health and disease. *Neth. Heart J.* **22**, 463–469
30. Kentish, J. C., McCloskey, D. T., Layland, J., Palmer, S., Leiden, J. M., Martin, A. F., *et al.* (2001) Phosphorylation of troponin I by protein kinase A accelerates relaxation and crossbridge cycle kinetics in mouse ventricular muscle. *Circ. Res.* **88**, 1059–1065
31. Takimoto, E., Soergel, D. G., Janssen, P. M., Stull, L. B., Kass, D. A., and Murphy, A. M. (2004) Frequency- and afterload-dependent cardiac modulation in vivo by troponin I with constitutively active protein kinase A phosphorylation sites. *Circ. Res.* **94**, 496–504
32. Zhang, R., Zhao, J., Mandveno, A., and Potter, J. D. (1995) Cardiac troponin I phosphorylation increases the rate of cardiac muscle relaxation. *Circ. Res.* **76**, 1028–1035
33. Tachampa, K., Wang, H., Farman, G. P., and de Tombe, P. P. (2007) Cardiac troponin I threonine 144: role in myofilament length dependent activation. *Circ. Res.* **101**, 1081–1083
34. Westfall, M. V., and Metzger, J. M. (2007) Single amino acid substitutions define isoform-specific effects of troponin I on myofilament Ca2+ and pH sensitivity. *J. Mol. Cell Cardiol.* **43**, 107–118
35. Kampourakis, T., Ponnam, S., Sun, Y. B., Sevrieva, I., and Irving, M. (2018) Structural and functional effects of myosin binding protein-C phosphorylation in heart muscle are not mimicked by serine-to-aspartate substitutions. *J. Biol. Chem.* **293**, 14270–14275
36. Bunch, T. A., Kanassatega, R. S., Lepak, V. C., and Colson, B. A. (2019) Human cardiac myosin-binding protein C restricts actin structural dynamics in a cooperative and phosphorylation-sensitive manner. *J. Biol. Chem.* **294**, 16228–16240
37. Martin-Garrido, A., Biesiadecki, B. J., Salhi, H. E., Shaifta, Y., Dos Remedios, C. G., Ayaz-Guner, S., *et al.* (2018) Monophosphorylation of cardiac troponin-I at Ser-23/24 is sufficient to regulate cardiac myofibrillar Ca(2+) sensitivity and calpain-induced proteolysis. *J. Biol. Chem.* **293**, 8588–8599
38. Zhang, R., Zhao, J., and Potter, J. D. (1995) Phosphorylation of both serine residues in cardiac troponin I is required to decrease the Ca2+ affinity of cardiac troponin C. *J. Biol. Chem.* **270**, 30773–30780
39. Wijnker, P. J., Foster, D. B., Tsao, A. L., Frazier, A. H., dos Remedios, C. G., Murphy, A. M., *et al.* (2013) Impact of site-specific phosphorylation of protein kinase A sites Ser23 and Ser24 of cardiac troponin I in human cardiomyocytes. *Am. J. Physiol. Heart Circ. Physiol.* **304**, H260–268
40. Messer, A. E., Gallon, C. E., McKenna, W. J., Dos Remedios, C. G., and Marston, S. B. (2009) The use of phosphate-affinity SDS-PAGE to measure the cardiac troponin I phosphorylation site distribution in human heart muscle. *Proteomics Clin. Appl.* **3**, 1371–1382
41. Kinoshita, E., Kinoshita-Kikuta, E., Takiyama, K., and Koike, T. (2006) Phosphate-binding tag, a new tool to visualize phosphorylated proteins. *Mol. Cell Proteomics* **5**, 749–757
42. Kobayashi, T., Yang, X., Walker, L. A., Van Breemen, R. B., and Solaro, R. J. (2005) A non-equilibrium isoelectric focusing method to determine states of phosphorylation of cardiac troponin I: Identification of ser-23 and ser-24 as significant sites of phosphorylation by protein kinase C. *J. Mol. Cell Cardiol.* **38**, 213–218
43. Sevrieva, I. R., Brandmeier, B., Ponnam, S., Gautel, M., Irving, M., Campbell, K. S., *et al.* (2020) Cardiac myosin regulatory light chain kinase modulates cardiac contractility by phosphorylating both myosin regulatory light chain and troponin I. *J. Biol. Chem.* **295**, 4398–4410
44. Blumenthal, D. K., Stull, J. T., and Gill, G. N. (1978) Phosphorylation of cardiac troponin by guanosine 3':5'-monophosphate-dependent protein kinase. *J. Biol. Chem.* **253**, 324–326
45. Zhang, J., Guy, M. J., Norman, H. S., Chen, Y. C., Xu, Q., Dong, X., *et al.* (2011) Top-down quantitative proteomics identified phosphorylation of cardiac troponin I as a candidate biomarker for chronic heart failure. *J. Proteome Res.* **10**, 4054–4065
46. Mamidi, R., Gresham, K. S., Verma, S., and Stelzer, J. E. (2016) Cardiac myosin binding protein-C phosphorylation modulates myofilament length-dependent activation. *Front. Physiol.* **7**, 38
47. Kampourakis, T., Yan, Z., Gautel, M., Sun, Y. B., and Irving, M. (2014) Myosin binding protein-C activates thin filaments and inhibits thick filaments in heart muscle cells. *Proc. Natl. Acad. Sci. U. S. A.* **111**, 18763–18768
48. Sun, Y. B., Lou, F., and Irving, M. (2009) Calcium- and myosin-dependent changes in troponin structure during activation of heart muscle. *J. Physiol.* **587**, 155–163
49. Allen, D. G., and Kurihara, S. (1980) Calcium transients in mammalian ventricular muscle. *Eur. Heart J.* https://doi.org/10.1093/eurheartj/1.suppl_1.5
50. Fabiato, A. (1981) Myoplasmic free calcium concentration reached during the twitch of an intact isolated cardiac cell and during calcium-induced release of calcium from the sarcoplasmic reticulum of a skinned cardiac cell from the adult rat or rabbit ventricle. *J. Gen. Physiol.* **78**, 457–497
51. Dibb, K. M., Eisner, D. A., and Trafford, A. W. (2007) Regulation of systolic [Ca2+]i and cellular Ca2+ flux balance in rat ventricular myocytes by SR Ca2+, L-type Ca2+ current and diastolic [Ca2+]i. *J. Physiol.* **585**, 579–592
52. Frampton, J. E., Orchard, C. H., and Boyett, M. R. (1991) Diastolic, systolic and sarcoplasmic reticulum [Ca2+] during inotropic interventions in isolated rat myocytes. *J. Physiol.* **437**, 351–375
53. Sankaranarayanan, R., Kistamas, K., Greensmith, D. J., Venetucci, L. A., and Eisner, D. A. (2017) Systolic [Ca(2+)]i regulates diastolic levels in rat ventricular myocytes. *J. Physiol.* **595**, 5545–5555
54. Eisner, D. A., Caldwell, J. L., Kistamas, K., and Trafford, A. W. (2017) Calcium and excitation-contraction coupling in the heart. *Circ. Res.* **121**, 181–195
55. Robertson, I. M., Sevrieva, I., Li, M. X., Irving, M., Sun, Y. B., and Sykes, B. D. (2015) The structural and functional effects of the familial

hypertrophic cardiomyopathy-linked cardiac troponin C mutation, L29Q. *J. Mol. Cell Cardiol.* **87**, 257–269
56. Luther, P. K., Winkler, H., Taylor, K., Zoghbi, M. E., Craig, R., Padrón, R., *et al.* (2011) Direct visualization of myosin-binding protein C bridging myosin and actin filaments in intact muscle. *Proc. Natl. Acad. Sci. U. S. A.* **108**, 11423–11428
57. Reconditi, M., Brunello, E., Fusi, L., Linari, M., Martinez, M. F., Lombardi, V., *et al.* (2014) Sarcomere-length dependence of myosin filament structure in skeletal muscle fibres of the frog. *J. Physiol.* **592**, 1119–1137
58. Mun, J. Y., Previs, M. J., Yu, H. Y., Gulick, J., Tobacman, L. S., Beck Previs, S., *et al.* (2014) Myosin-binding protein C displaces tropomyosin to activate cardiac thin filaments and governs their speed by an independent mechanism. *Proc. Natl. Acad. Sci. U. S. A.* **111**, 2170–2175
59. Risi, C., Belknap, B., Forgacs-Lonart, E., Harris, S. P., Schröder, G. F., White, H. D., *et al.* (2018) N-terminal domains of cardiac myosin binding protein C cooperatively activate the thin filament. *Structure* **26**, 1604–1611.e1604
60. Shaffer, J. F., Kensler, R. W., and Harris, S. P. (2009) The myosin-binding protein C motif binds to F-actin in a phosphorylation-sensitive manner. *J. Biol. Chem.* **284**, 12318–12327
61. Ponnam, S., Sevrieva, I., Sun, Y. B., Irving, M., and Kampourakis, T. (2019) Site-specific phosphorylation of myosin binding protein-C coordinates thin and thick filament activation in cardiac muscle. *Proc. Natl. Acad. Sci. U. S. A.* **116**, 15485–15494
62. Hwang, P. M., Cai, F., Pineda-Sanabria, S. E., Corson, D. C., and Sykes, B. D. (2014) The cardiac-specific N-terminal region of troponin I positions the regulatory domain of troponin C. *Proc. Natl. Acad. Sci. U. S. A.* **111**, 14412–14417
63. Marston, S. (2022) Recent studies of the molecular mechanism of lusitropy due to phosphorylation of cardiac troponin I by protein kinase A. *J. Muscle Res. Cell Motil.* https://doi.org/10.1007/s10974-022-09630-4
64. Wattanapermpool, J., Guo, X., and Solaro, R. J. (1995) The unique amino-terminal peptide of cardiac troponin I regulates myofibrillar activity only when it is phosphorylated. *J. Mol. Cell Cardiol.* **27**, 1383–1391
65. Robertson, S. P., Johnson, J. D., Holroyde, M. J., Kranias, E. G., Potter, J. D., and Solaro, R. J. (1982) The effect of troponin I phosphorylation on the Ca2+-binding properties of the Ca2+-regulatory site of bovine cardiac troponin. *J. Biol. Chem.* **257**, 260–263
66. Dong, W. J., Jayasundar, J. J., An, J., Xing, J., and Cheung, H. C. (2007) Effects of PKA phosphorylation of cardiac troponin I and strong cross-bridge on conformational transitions of the N-domain of cardiac troponin C in regulated thin filaments. *Biochemistry* **46**, 9752–9761
67. van Dijk, S. J., Dooijes, D., dos Remedios, C., Michels, M., Lamers, J. M., Winegrad, S., *et al.* (2009) Cardiac myosin-binding protein C mutations and hypertrophic cardiomyopathy: haploinsufficiency, deranged phosphorylation, and cardiomyocyte dysfunction. *Circulation* **119**, 1473–1483
68. Barefield, D., and Sadayappan, S. (2010) Phosphorylation and function of cardiac myosin binding protein-C in health and disease. *J. Mol. Cell Cardiol.* **48**, 866–875
69. Vikhorev, P. G., Vikhoreva, N. N., Yeung, W., Li, A., Lal, S., dos Remedios, C. G., *et al.* (2022) Titin-truncating mutations associated with dilated cardiomyopathy alter length-dependent activation and its modulation *via* phosphorylation. *Cardiovasc. Res.* **118**, 241–253
70. van der Velden, J., de Jong, J. W., Owen, V. J., Burton, P. B., and Stienen, G. J. (2000) Effect of protein kinase A on calcium sensitivity of force and its sarcomere length dependence in human cardiomyocytes. *Cardiovasc. Res.* **46**, 487–495
71. Kooij, V., Saes, M., Jaquet, K., Zaremba, R., Foster, D. B., Murphy, A. M., *et al.* (2010) Effect of troponin I Ser23/24 phosphorylation on Ca2+-sensitivity in human myocardium depends on the phosphorylation background. *J. Mol. Cell Cardiol.* **48**, 954–963
72. Harris, S. P., Belknap, B., Van Sciver, R. E., White, H. D., and Galkin, V. E. (2016) C0 and C1 N-terminal Ig domains of myosin binding protein C exert different effects on thin filament activation. *Proc. Natl. Acad. Sci. U. S. A.* **113**, 1558–1563
73. Mamidi, R., Gollapudi, S. K., Mallampalli, S. L., and Chandra, M. (2012) Alanine or aspartic acid substitutions at serine23/24 of cardiac troponin I decrease thin filament activation, with no effect on crossbridge detachment kinetics. *Arch. Biochem. Biophys.* **525**, 1–8
74. Jin, J. P., Walsh, M. P., Sutherland, C., and Chen, W. (2000) A role for serine-175 in modulating the molecular conformation of calponin. *Biochem. J.* **350 Pt 2**, 579–588
75. Hunter, T. (2012) Why nature chose phosphate to modify proteins. *Philos. Trans. R. Soc. Lond. B Biol. Sci.* **367**, 2513–2516
76. Bardswell, S. C., Cuello, F., Rowland, A. J., Sadayappan, S., Robbins, J., Gautel, M., *et al.* (2010) Distinct sarcomeric substrates are responsible for protein kinase D-mediated regulation of cardiac myofilament Ca2+ sensitivity and cross-bridge cycling. *J. Biol. Chem.* **285**, 5674–5682
77. Memo, M., Leung, M. C., Ward, D. G., dos Remedios, C., Morimoto, S., Zhang, L., *et al.* (2013) Familial dilated cardiomyopathy mutations uncouple troponin I phosphorylation from changes in myofibrillar Ca(2)(+) sensitivity. *Cardiovasc. Res.* **99**, 65–73
78. van der Velden, J., Papp, Z., Zaremba, R., Boontje, N., Dejong, J., Owen, V., *et al.* (2003) Increased Ca2+-sensitivity of the contractile apparatus in end-stage human heart failure results from altered phosphorylation of contractile proteins. *Cardiovasc. Res.* **57**, 37–47
79. Solaro, R. J., and Kobayashi, T. (2011) Protein phosphorylation and signal transduction in cardiac thin filaments. *J. Biol. Chem.* **286**, 9935–9940
80. Liu, Y., Chen, J., Fontes, S. K., Bautista, E. N., and Cheng, Z. (2022) Physiological and pathological roles of protein kinase A in the heart. *Cardiovasc. Res.* **118**, 386–398
81. Hanft, L. M., Cornell, T. D., McDonald, C. A., Rovetto, M. J., Emter, C. A., and McDonald, K. S. (2016) Molecule specific effects of PKA-mediated phosphorylation on rat isolated heart and cardiac myofibrillar function. *Arch. Biochem. Biophys.* **601**, 22–31
82. Al-Khayat, H. A., Kensler, R. W., Squire, J. M., Marston, S. B., and Morris, E. P. (2013) Atomic model of the human cardiac muscle myosin filament. *Proc. Natl. Acad. Sci. U. S. A.* **110**, 318–323
83. Inchingolo, A. V., Previs, S. B., Previs, M. J., Warshaw, D. M., and Kad, N. M. (2019) Revealing the mechanism of how cardiac myosin-binding protein C N-terminal fragments sensitize thin filaments for myosin binding. *Proc. Natl. Acad. Sci. U. S. A.* **116**, 6828–6835
84. Moss, R. L., Razumova, M., and Fitzsimons, D. P. (2004) Myosin cross-bridge activation of cardiac thin filaments: Implications for myocardial function in health and disease. *Circ. Res.* **94**, 1290–1300
85. Kampourakis, T., Zhang, X., Sun, Y. B., and Irving, M. (2018) Omecamtiv mercabil and blebbistatin modulate cardiac contractility by perturbing the regulatory state of the myosin filament. *J. Physiol.* **596**, 31–46
86. Lynch, T. L.t., Kumar, M., McNamara, J. W., Kuster, D. W. D., Sivaguru, M., Singh, R. R., *et al.* (2021) Amino terminus of cardiac myosin binding protein-C regulates cardiac contractility. *J. Mol. Cell Cardiol.* **156**, 33–44
87. Wijnker, P. J., Sequeira, V., Foster, D. B., Li, Y., Dos Remedios, C. G., Murphy, A. M., *et al.* (2014) Length-dependent activation is modulated by cardiac troponin I bisphosphorylation at Ser23 and Ser24 but not by Thr143 phosphorylation. *Am. J. Physiol. Heart Circ. Physiol.* **306**, H1171–1181
88. Hanft, L. M., Fitzsimons, D. P., Hacker, T. A., Moss, R. L., and McDonald, K. S. (2021) Cardiac MyBP-C phosphorylation regulates the Frank-Starling relationship in murine hearts. *J. Gen. Physiol.* **153**
89. Cimiotti, D., Fujita-Becker, S., Möhner, D., Smolina, N., Budde, H., Wies, A., *et al.* (2020) Infantile restrictive cardiomyopathy: cTnI-R170G/W impair the interplay of sarcomeric proteins and the integrity of thin filaments. *PLoS One* **15**, e0229227
90. Risi, C., Schäfer, L. U., Belknap, B., Pepper, I., White, H. D., Schröder, G. F., *et al.* (2021) High-resolution cryo-EM structure of the cardiac Actomyosin complex. *Structure* **29**, 50–60.e54
91. Kampourakis, T., and Irving, M. (2015) Phosphorylation of myosin regulatory light chain controls myosin head conformation in cardiac muscle. *J. Mol. Cell Cardiol.* **85**, 199–206
92. Yamasaki, R., Wu, Y., McNabb, M., Greaser, M., Labeit, S., and Granzier, H. (2002) Protein kinase A phosphorylates titin's cardiac-specific N2B

domain and reduces passive tension in rat cardiac myocytes. *Circ. Res.* **90**, 1181–1188
93. Kruger, M., and Linke, W. A. (2006) Protein kinase-A phosphorylates titin in human heart muscle and reduces myofibrillar passive tension. *J. Muscle Res. Cell Motil.* **27**, 435–444
94. Chung, J. H., Biesiadecki, B. J., Ziolo, M. T., Davis, J. P., and Janssen, P. M. (2016) Myofilament calcium sensitivity: role in regulation of *in vivo* cardiac contraction and relaxation. *Front. Physiol.* **7**, 562
95. Eisner, D. A., Caldwell, J. L., Trafford, A. W., and Hutchings, D. C. (2020) The control of diastolic calcium in the heart: basic mechanisms and functional implications. *Circ. Res.* **126**, 395–412
96. Kampourakis, T., and Irving, M. (2021) The regulatory light chain mediates inactivation of myosin motors during active shortening of cardiac muscle. *Nat. Commun.* **12**, 5272
97. Dale, R. E., Hopkins, S. C., an der Heide, U. A., Marszałek, T., Irving, M., and Goldman, Y. E. (1999) Model-independent analysis of the orientation of fluorescent probes with restricted mobility in muscle fibers. *Biophys. J.* **76**, 1606–1618
98. Kampourakis, T., Ponnam, S., and Irving, M. (2018) Hypertrophic cardiomyopathy mutation R58Q in the myosin regulatory light chain perturbs thick filament-based regulation in cardiac muscle. *J. Mol. Cell Cardiol.* **117**, 72–81